CLUSTERS OF GALAXIES AND THE COSMIC LIGHT

Thesis by

Stephen Alan Shectman

In Partial Fulfillment of the Requirements

for the Degree of

Doctor of Philosophy

California Institute of Technology

Pasadena, California

1974

(Submitted June 28, 1973)

ACKNOWLEDGEMENTS

To the multitude whose efforts contributed to the success of this investigation, my heartfelt thanks. In particular, I would like to express my gratitude

To my advisor, Professor James E. Gunn, for more than just the valuable guidance he has provided throughout the course of this research,

To Professor J.B. Oke, for his support in constructing the plate scanner and for numerous helpful conversations,

To Professor Jesse Greenstein, for his insight, advice and understanding,

To my colleagues Greg Shields, Bob Kirshner, Barry Turnrose, Ken Braly and especially Gus Oemler, for many things but above all for their gift of friendship,

To the Hale Observatories for providing the facilities which made this investigation possible, and to the Palomar mountain staff, especially Mr. Dennis Palm, for their support in obtaining the observations,

To the Alfred P. Sloan Research Foundation, for the grant to build the microphotometer data system, and to Dr. Edwin Dennison and the Astro-Electronics Laboratory

for its construction and maintenance,

To the National Science Foundation for a Graduate Fellowship and for much of the support for the data reduction,

And finally to Robin, for love and understanding, without whom I insist that none of this would have been possible.

When stars were born, they stood and stared
about the sky and wondered where
in all that night there might have been
someone to praise and study them.
"What good is it" they asked aloud,
"to stand here, silver, fair and proud
when no one sees and no one knows?"
the simple stars rehearsed their woes
until at last the Night agreed
to see if it might mend their need
and fashioned from the cosmic dust
a creature very curious,
with eyes to see and soul to praise
the stars' celestial wondrous ways;
with mind to know and heart to care
for skies and all that happens there.

-- Robin Shectman

ABSTRACT

Because galaxies cluster in space, the cosmic background light due to galaxies is not smoothly distributed on the night sky. Part I predicts spatial power spectra for the cosmic light fluctuations, based on the luminosity function for nearby galaxies and on the clumpiness of the galaxy distribution derived from galaxy counts. Part II describes a measurement of the spatial power spectrum of the cosmic light on a series of photographic plates taken with the Palomar 48-inch (122cm) Schmidt camera. This power spectrum is interpreted to provide a measure of the covariance of the galaxy distribution and the mean emissivity of galaxies in space.

TABLE OF CONTENTS

THE ASTROPHYSICAL JOURNAL, 179:681–698, 1973 February 1

CLUSTERS OF GALAXIES AND THE COSMIC LIGHT*

STEPHEN A. SHECTMAN
Hale Observatories, California Institute of Technology, Carnegie Institution of Washington
Received 1972 June 23

ABSTRACT

Because galaxies cluster in space, the cosmic background light due to galaxies is not smoothly distributed on the night sky. Based on an explicit description of clusters of galaxies, spatial power spectra for the cosmic-light fluctuations are predicted. These spectra depend strongly on the luminosity density of the universe and the covariance structure of the galaxy distribution. They also depend somewhat on cosmological model.

Subject headings: cosmic background radiation — cosmology — galaxies, clusters of

I. INTRODUCTION

The total light of the night sky from distant sources has long been a subject of interest. The resolution to Olbers' paradox, that the sky would appear blazingly bright in an infinite Euclidean universe homogeneously populated with stars, was provided by the discovery of interstellar absorption and the finite extent of the Milky Way. The same situation with regard to the extragalactic nebulae is avoided in the non-Euclidean cosmologies of general relativity and other metric theories of gravity.

Indeed, although the extragalactic cosmic background has been detected in the radio and X-ray regions of the spectrum, the expanding universe has reduced the optical background due to distant galaxies to a small fraction of the nightsky intensity from aurora, airglow, and zodiacal light. Estimates by many authors, most recently Sandage and Tammann (1964) and Gunn (1965), place the mean cosmic light lower than 1 percent of the total nightsky intensity under favorable conditions. Ground-based attempts to measure the mean extragalactic light would appear extremely difficult if not futile.

With the advent of Schmidt cameras, Zwicky (1957) remarked upon the truly extensive clustering of galaxies in space. This phenomenon has been statistically characterized by Neyman, Scott, and Shane (1953), Limber (1954), and again by Gunn (1965), utilizing the data from galaxy counts. In the context of a very complete statistical theory of the distribution of galaxies in space, Gunn (1965) made the first predictions regarding the statistical structure of the cosmic light due to clusters of galaxies. Because one would expect the long-term average of the atmospheric and solar-system contributions to the nightsky brightness to be very smooth indeed, there appears to be some hope to distinguish the spatial fluctuations of the cosmic light as distinct from the mean background.

The present study parallels closely that of Gunn except that the clustering of galaxies is viewed explicitly rather than described strictly as a statistical process.

Until such time as the dust has had a chance to settle upon some new canonical value of the Hubble constant, it seems wiser to adopt the convenient value $H_0 = 100$ km s^{-1} Mpc^{-1}, on which all of the calculations in this paper are based. One can show, however, that the predictions for directly observable quantities, specifically for the cosmic-light intensity and its spatial power spectrum, are independent of the choice of Hubble constant.

* Supported in part by the National Science Foundation [GP-27304, GP-28027].

II. THE DISTRIBUTION OF GALAXIES IN SPACE

Consider for the moment a probability density function $F(\mathbf{r})$ which governs the distribution of galaxies in space, with

$$\frac{1}{V}\int_V F(\mathbf{r})d^3\mathbf{r} = 1$$

for a suitably large volume. That is, if the mean density of galaxies in space is Λ, the probability that a galaxy exists at $\mathbf{r}$ is $\Lambda F(\mathbf{r})$. If we make the assumption that light emission in the universe follows this same distribution, then the probable emissivity at any point is $\epsilon_\nu F(\mathbf{r})$, where ϵ_ν is the mean emissivity of space.

In fact, the true distribution of galaxies in space is a particular discrete realization of this random process. If Λ were made larger and larger, the actual number of galaxies observed in any finite volume would follow more and more closely the probability function $F(\mathbf{r})$.

This probability distribution generates a covariance density

$$G(x) = \frac{1}{V}\int_V F(\mathbf{r})F(\mathbf{r} + x)d^3\mathbf{r}\,,$$

which describes the correlation of the probability from one point in space to the next. In particular,

$$G(0) = \langle F^2(\mathbf{r})\rangle$$

is the mean square of the spatial probability distribution.

If we were to consider the actual discrete distribution of galaxies in space, the probability distribution would consist of a series of δ-functions at the site of each galaxy, and the covariance would contain a term

$$G(x) = \frac{1}{V}\int_V \delta(\mathbf{r})\delta(\mathbf{r} + x)d^3\mathbf{r} = \frac{1}{V}\delta(x)$$

for each galaxy in the volume. Thus we may view the actual covariance as consisting of a continuous component due to the correlation from volume to volume of the probability that a galaxy exists in any volume, and a singular contribution due to the discrete realization of the process.

Alternatively the correlation structure of the distribution may be described by the power spectral density, the Fourier transform of the covariance:

$$S(k) = \frac{1}{(2\pi)^3}\int G(x)\exp(-ik\cdot x)d^3x\,.$$

The normalization has been chosen so that the covariance is in turn

$$G(x) = \int S(k)\exp(ik\cdot x)d^3k$$

and particularly

$$G(0) = \int S(k)d^3k\,.$$

If we imagine that the galaxy distribution $F(r)$ is identically zero outside the large volume V, we may write the power spectrum as

$$S(k) = \frac{1}{(2\pi)^3}\int_V \frac{1}{V}\int_V F(r)F(r+x)d^3r \exp(-ik\cdot x)d^3x$$

$$= \frac{1}{(2\pi)^3 V}\int_V F(r)\int_V F(x)\exp[-ik\cdot(x-r)]d^3x d^3r$$

$$= \frac{1}{(2\pi)^3 V}\int_V F(r)\exp(ik\cdot r)d^3r \int_V F(x)\exp(-ik\cdot x)d^3x ,$$

but the two integrals are complex conjugates, hence the result of the convolution theorem:

$$S(k) = \frac{1}{(2\pi)^3 V}\left|\int_V F(r)\exp(-ik\cdot r)d^3r\right|^2 .$$

We require a relation between the three-dimensional properties of the galaxy distribution $G(x)$ and $S(k)$ and the two-dimensional covariance and power spectrum of the distribution as it is seen in projection on the sky. Consider the power spectrum of a slab of volume V of the galaxy distribution projected on a plane of area A. In Cartesian coordinates $\rho = (r_1, r_2)$ and $r = (\rho, r_3)$ the probability density viewed along r_3,

$$f(\rho) = \int_{\Delta r_3} F(r)dr_3 ,$$

generates the power spectral density

$$s(\varkappa) = \frac{1}{(2\pi)^2 A}\left|\int_A f(\rho)\exp(-i\varkappa\cdot\rho)d^2\rho\right|^2 .$$

But

$$S(\varkappa, k_3 = 0) = \frac{1}{(2\pi)^3 V}\left|\int_A\int_{\Delta r_3} F(\rho, r_3)dr_3 \exp(-i\varkappa\cdot\rho)d^2\rho\right|^2 ,$$

so that

$$s(\varkappa) = \frac{2\pi V}{A}S(\varkappa, 0) .$$

The power spectrum of the projected distribution can be expressed in terms of the covariance of the projected distribution as

$$s(\varkappa) = \frac{1}{(2\pi)^2}\int g(\chi)\exp(-i\varkappa\cdot\chi)d^2\chi ;$$

and since

$$S(\varkappa, 0) = \frac{1}{(2\pi)^3}\int\int G(\chi, x_3)dx_3 \exp(-i\varkappa\cdot\chi)d^2\chi ,$$

$$s(\varkappa) = \frac{V}{(2\pi)^2 A}\int\int G(\chi, x_3)dx_3 \exp(-i\varkappa\cdot\chi)d^2\chi ,$$

the covariance of the distribution in projection becomes

$$g(\chi) = \frac{V}{A} \int G(\chi, x_3) dx_3 .$$

In order to calculate the power spectrum of the cosmic light on an area of the sphere small enough to be considered flat, it is only necessary to add up the contributions from the power spectra of a series of such volumes seen in projection along the line of sight. To do so, however, the non-Euclidean nature of the space along the line of sight must be taken into account.

III. COSMOLOGICAL CONSIDERATIONS

The observational consequences of the Friedmann cosmologies, solutions to the general-relativistic field equations in an isotropic, homogeneous universe, have been discussed by many authors (see, for example, Sandage 1961). We merely present those results of the theory, with the additional restriction to vanishing cosmological constant, most important to the issue at hand.

Thus, the Robertson-Walker line element may be written

$$ds^2 = -c^2 d\tau^2 + R^2(\tau)[du^2 + \sigma^2(u) d\Omega^2] ,$$

where $R(\tau)$ is a scale factor which evolves with cosmic time τ. For a radial light track $ds^2 = d\Omega^2 = 0$, so that

$$u = c \int_{\tau_1}^{\tau_0} \frac{d\tau}{R(\tau)}$$

is a dimensionless distance from an emitter at time τ_1 to an observer at τ_0. The function $\sigma(u)$ becomes sinh (u), u, or sin (u) for hypersurfaces of constant cosmic time of negative, zero, or positive curvature, respectively.

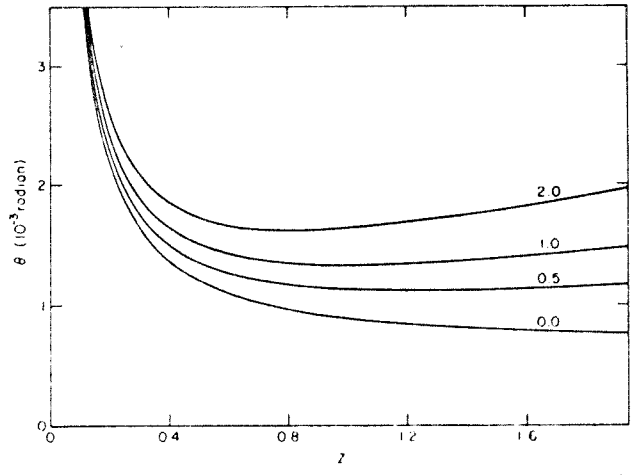

FIG. 1.—Apparent angular size subtended by an object of constant length $l = 1$ Mpc perpendicular to the line of sight, as a function of redshift z, for values of $q_0 = 0.0$, 0.5, 1.0, and 2.0.

The present area of a sphere of radius u is shown from the line element to be $4\pi R_0^2\sigma^2(u)$. Then the flux observed at ν_0 from a source of specific luminosity L_{ν_1} at the frequency of emission is given by

$$f_{\nu_0} = \frac{L_{\nu_1}}{4\pi R_0^2\sigma^2(u_1)(1+z)},$$

where one of the factors of $(1+z)$ contained in the familiar formula for bolometric luminosity has been absorbed by the change in bandpass from $d\nu_1$ to $d\nu_0$.

Similarly, the observed angular diameter of an object of width l at distance u_1 becomes

$$\theta = \frac{l}{R_1\sigma(u_1)}.$$

Figure 1 presents the dependence on distance of the angular diameter of an object of constant l, for various values of q_0. The apparent angular size varies slowly beyond $z = 0.5$, and, except for the case $q_0 = 0$, in fact begins to grow with increasing distance. This effect is responsible for much of the dependence on cosmology of the spatial power spectrum of the cosmic light, especially if the clustering of galaxies is characterized chiefly by a single scale length.

IV. THE MEAN COSMIC LIGHT

Consider the contribution to the average extragalactic background from the dimensionless increment of distance du. If the mean emissivity (ergs s^{-1} cm^{-3} Hz^{-1}) of the universe is locally ϵ_ν, and if we neglect evolutionary effects, the emissivity at distance $u(z)$ along the line of sight will be $\epsilon_\nu(1+z)^3$. The volume of a shell of thickness du and 1 steradian apparent solid angle will be $R_1^3\sigma^2(u_1)du_1$. The luminosity of this shell is then

$$dL_{\nu_1} = \epsilon_{\nu_1}(1+z)^3R_1^3\sigma^2(u_1)du_1;$$

and the contribution to the mean cosmic-light intensity (ergs s^{-1} cm^{-2} $sterad^{-1}$ Hz^{-1}) from this shell becomes

$$dI_{\nu_0} = \frac{\epsilon_{\nu_1}(1+z)^3R_1^3\sigma^2(u_1)du_1}{4\pi R_0^2\sigma^2(u_1)(1+z)},$$

$$dI_{\nu_0} = \frac{\epsilon_{\nu_1}R_1du_1}{4\pi}.$$

In order to estimate ϵ_ν, we make the assumption that all of the emissivity at optical wavelengths is provided by galaxies, since searches for other sources of optical emission at the present epoch—for example, a continuous background light in rich clusters of galaxies—have yielded somewhat ambiguous results.

Early surveys of galaxies—for example, by Hubble (1936)—were interpreted in terms of a Gaussian distribution of galaxy absolute magnitudes with very low dispersion, less than 1 mag. More recent studies—e.g., those by Kiang (1961) and Shapiro (1971)—indicate a considerably broader differential luminosity function which continues to rise at faint magnitudes, and which agrees well in shape with the luminosity function found by Abell (1962) and others for rich clusters of galaxies.

We base our estimates for the cosmic light on the luminosity function suggested by Kiang (1961):

$$\phi(M_{pg}) = a(M - M_0)^3 \qquad (0.0 < M - M_0 < 2.5)$$

$$= a\left(\frac{2.5^3}{10^{0.5}}\right)10^{0.2(M-M_0)} \qquad (2.5 < M - M_0 < 8.0).$$

The exponential rise at faint magnitudes is not fast enough to overcome the decrease in luminosity $10^{-0.4M}$. We will restrict our predictions to the emission arising in the interval $0 < M - M_0 < 8.0$ since there is little evidence regarding the extension of the luminosity function to fainter magnitudes. The additional luminosity density generated by extrapolation of the exponential to arbitrarily faint magnitudes is less than 10 percent.

To the suggested value of $M_0 = -22.0$ mag in the photographic band, the following corrections are applied: (1) +0.22 mag average internal absorption (Holmberg 1958); (2) +0.25 mag for the assumed obscuration at the galactic poles; (3) +0.14 mag to the *B*-magnitude system; so that the revised value of M_0 in the *B* system is −21.39 mag. The value for the normalization

$$a = 10^{-2.94} \text{ galaxy Mpc}^{-3} \text{ mag}^{-1}$$

yields a constant C_{pg} in the count relation

$$\log N(m) = 0.6m + C$$

of −8.91, which agrees well with the value −8.87 obtained by Holmberg (1958).

Two precautions are in order regarding this luminosity function. The first concerns the great difficulty involved in even defining the magnitude of a galaxy, for which the total luminosity converges to a limit only very slowly as greater and greater areas around the galaxian image are taken into account. The magnitudes involved are based upon the conventions of Holmberg (1958) and Humason, Mayall, and Sandage (1956, hereafter HMS), who define the magnitude of a galaxy within some standard limiting isophote which is substantially greater in extent than the apparent image on photographic prints such as those of the *Palomar Sky Survey*. The total magnitudes are nevertheless certain to be underestimates, but by how much is only a matter of opinion at the present time. We make no attempt to apply such a correction, but bear in mind that the derived luminosity density is likely to be 10 or 20 percent too low.

The other difficulty arises from the limited volume of space sampled to obtain the luminosity function. The survey of galaxies involved is complete at best to apparent magnitude +13, so that for much of the range in absolute magnitude the radius of the sampled volume is effectively less than 20 Mpc. Because the distribution of galaxies in space is far from uniform, such a volume can hardly be considered representative of the universe as a whole. The well-known excess of bright galaxies in the northern galactic hemisphere as compared to the southern may be one manifestation of this effect.

With these qualifications in mind, we require only the spectral dependence of the light emitted by galaxies to arrive at the mean emissivity per unit frequency ϵ_ν. Although much work has been done on the detailed spectral energy distribution for giant elliptical and S0 galaxies, little more than the average color index is known for later-type spiral and irregular galaxies.

We divide galaxies into three broad classes; ellipticals and lenticulars (E and S0), early spirals (Sa and Sb), and late spirals and irregulars (Sc and Irr). There is some justification (HMS 1956; Christiansen 1968) for the rough assumption that the

TABLE 1

PROPERTIES OF THREE BROAD CLASSES OF GALAXIES

Type	Percent of Total	$B - V$	ν_0 (10^{14} Hz)
E, S0.....	31.2	0.95	1.10
Sa, Sb.....	25.6	0.75	1.30
Sc, Irr.....	43.2	0.50	1.70

luminosity function for all the types is the same in the B bandpass, although this clearly will not be true in other regions of the spectrum. We adopt a form for the spectral energy distribution suggested by Gunn (1965)

$$L_\nu = \frac{L_0}{2\nu_0}\left(\frac{\nu}{\nu_0}\right)^2 \exp\left(-\nu/\nu_0\right),$$

where ν_0 is matched to the observed color index for a given class of galaxies.

Table 1 summarizes the properties of each of the three classes of galaxies. The fraction of galaxies of each type is taken from a study of the luminosity function by Christensen (1968), and agrees well with the proportions given by Hubble (1936) and Sandage (1961) for samples selected by apparent magnitude.

The spectral dependence for each class is presented in figure 2. The spectral energy distribution found by Oke and Schild (1971) for giant elliptical and S0 galaxies in the Virgo cluster has been plotted along the curve for $\nu_0 = 1.1 \times 10^{14}$ Hz. The fit is reasonable from 6500 Å to 4000 Å, but becomes poor shortward of 4000 Å where the effects of line blanketing become pronounced. When similarly detailed data become available for spiral galaxies, calculations based directly on the scans will represent a considerable improvement in this respect.

Table 2 presents the mean emissivity for galaxies derived from the results above. Using the absolute photometric calibration of Oke and Schild (1970), the Kiang

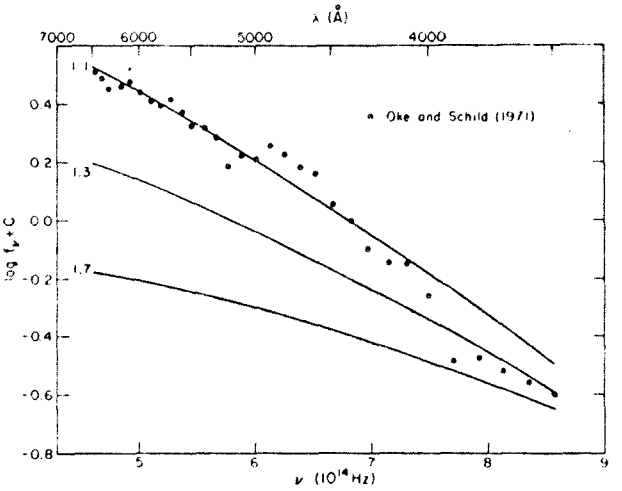

FIG. 2.—Adopted spectral energy distributions for three broad classes of galaxies ($\nu_0 = 1.1$, 1.3, and 1.7×10^{14} Hz).

TABLE 2

MEAN SPECIFIC EMISSIVITY OF GALAXIES
(10^{-47} ergs s^{-1} cm^{-3} Hz^{-1})

λ (Å)	ϵ_ν	λ (Å)	ϵ_ν
3500.....	1.64	5500....	6.48
4000.....	2.69	6000....	7.70
4500.....	3.90	6500....	8.85
5000.....	5.19	7000....	9.84

luminosity function for the *B*-magnitude system was applied monochromatically at 4400 Å with the correction to other wavelengths calculated from the suggested spectral energy distribution for each class of galaxies. The emissivity is reduced to the north galactic pole but not to outside the galaxy.

Throughout the rest of this paper the predictions are restricted to a monochromatic received bandpass at 6500 Å. This wavelength is centered on the photo-red part of the spectrum just shortward of the marked increase in the brightness of the night sky in the near-infrared. Moreover, the bulk of the cosmic light received in this band originates in those regions of the visible spectrum for which the luminosity density due to galaxies is best determined.

In addition, the light from those galaxies brighter than some given red apparent magnitude is rejected in order to suppress a large local component to the cosmic light which is of no cosmological significance and which carries little information regarding the distribution of galaxies in space, at least for sample areas of modest size.

Table 3 lists the results for the mean cosmic-light intensity, under the assumption that the locally derived luminosity density applies along the entire line of sight. The effect on the mean light of a change in deceleration parameter q_0 from 0.0 to 2.0 is similar to the effect of lowering the cutoff magnitude from 17.0 to 20.0. Both result in a change in the cosmic light on the order of a factor of 2. These results agree well with the predictions of Sandage and Tammann (1964). For comparison the mean photo-red intensity of the night sky at Palomar is typically 4×10^{-18} ergs s^{-1} cm^{-2} $sterad^{-1}$ Hz^{-1}.

Figure 3 depicts in detail the contribution to the mean cosmic light from each increment along the line of sight. The bulk of the extragalactic optical background arises at redshifts between $z = 0.2$ and $z = 0.6$. Very little of the cosmic light arises at redshifts greater than $z = 1.0$. The effect of cosmology is not confined to the most distant component of the cosmic light but is rather evenly distributed along the line of sight.

TABLE 3

MEAN COSMIC-LIGHT INTENSITY AT 6500 Å
(10^{-20} ergs s^{-1} cm^{-2} $sterad^{-1}$ Hz^{-1})

	q_0 =			
$m_R >$	0	½	1	2
17.0.....	1.47	1.27	1.14	0.98
18.0.....	1.30	1.10	0.98	0.82
19.0.....	1.10	0.91	0.80	0.65
20.0.....	0.89	0.71	0.60	0.47

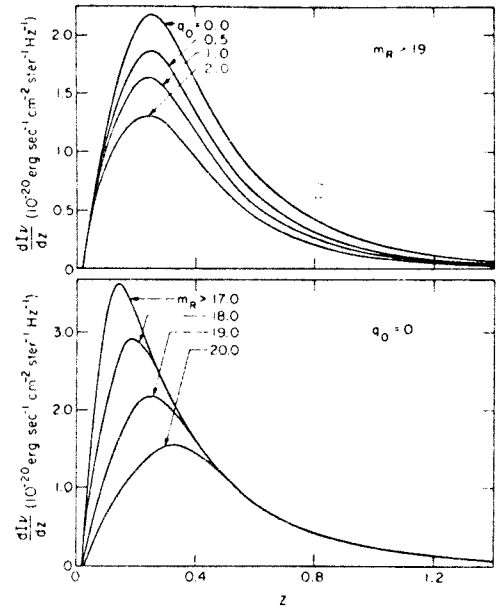

FIG. 3.—Differential contribution to the total cosmic-light intensity at 6500 Å from the increment in redshift dz, for several values of q_0 and rejection magnitude m_R.

V. CONTINUOUS COMPONENT OF THE POWER SPECTRUM

For simplicity, consider a cluster of galaxies with a Gaussian probability envelope. That is, for a cluster centered on the origin with expected population n, the probability density that a galaxy exists at any point is

$$F(r) = \frac{n}{(\pi l^2)^{3/2}} \exp(-r^2/l^2).$$

The length l will always be taken to be much smaller than the characteristic scale of the universe $R(\tau)$, so that on the scale of clusters of galaxies space may be considered essentially flat. Then the covariance density generated by this cluster will be

$$G(x) = \frac{1}{V}\int_V F(r)F(r+x)d^3r,$$

$$G(x) = \frac{1}{V}\frac{n^2}{(2\pi)^{3/2}l^3}\exp(-x^2/2l^2),$$

where V is an arbitrarily large volume. The length l is the correlation length of the cluster. Note that by calculating the covariance density for the cluster in isolation the mean of the distribution has been forced to zero.

Now suppose that the volume is in fact randomly populated with such clusters with a mean density ρ of cluster centers. Let the expected populations of the clusters follow some distribution function characterized by a mean square population $\langle n^2\rangle$. Then the

covariance density for each of the clusters adds, and since the volume contains ρV clusters, the actual covariance from the ensemble of clusters becomes

$$G(x) = \frac{\rho\langle n^2\rangle}{(2\pi)^{3/2}l^3}\exp(-x^2/2l^2).$$

If necessary, a variety of such ensembles for different correlation lengths could be added together in order to expand covariance densities of considerable complexity as a series of Gaussians.

This heuristic ensemble of clusters of galaxies exhibits all of the same second-moment properties that characterize any distribution of galaxies with this covariance behavior. At this point the explicit description of the distribution in terms of clusters is really unnecessary as long as one has at hand the spatial covariance density. Later, however, we will capitalize upon the similarity of this heuristic ensemble to the actual distribution of galaxies in space to estimate the error involved in sampling the statistical structure of the cosmic light over an area of restricted size.

If luminosity and number density are assumed to follow the same distribution in space, the covariance density of the luminosity distribution for the Gaussian cluster ensemble becomes

$$G(x) = \frac{\rho\langle L_\nu^2\rangle}{(2\pi)^{3/2}l^3}\exp(-x^2/2l^2),$$

where $\langle L_\nu^2\rangle$ is the mean square specific luminosity of a cluster. The covariance structure in this case is completely described by a correlation length l and a density contrast β

$$G(x) = \beta\epsilon_\nu^2\exp(-x^2/2l^2),$$

where the density contrast

$$\beta = \frac{\rho\langle L_\nu^2\rangle}{(2\pi)^{3/2}l^3\epsilon_\nu^2} = \frac{\rho\langle n^2\rangle}{(2\pi)^{3/2}l^3\Lambda^2}$$

(Λ is the mean number density of galaxies) is the same for both luminosity and number distributions.

At this point it is useful to express the covariance in terms of an auxiliary density ρ' which would be the density of clusters if they were all of the same intrinsic brightness:

$$\rho' = \rho\frac{\langle L_\nu^2\rangle}{\langle L_\nu\rangle^2} = \frac{1}{(2\pi)^{3/2}l^3\beta},$$

so that the covariance density becomes

$$G(x) = \frac{\rho'\langle L_\nu\rangle^2}{(2\pi)^{3/2}l^3}\exp(-x^2/2l^2).$$

By the result of § II, the covariance of the cosmic light for a volume V of the galaxy distribution projected on a plane of area A will be

$$g(\chi) = \frac{\sigma'\langle L_\nu\rangle^2}{2\pi l^2}\exp(-\chi^2/2l^2),$$

where $\sigma' = (V/A)\rho'$ is the auxiliary surface density of cluster centers in the plane. If the average luminosity of a cluster results in a flux at the Earth $\langle F_\nu\rangle$ and the cluster

correlation-length appears as an angle θ on the sky, the covariance density of the cosmic light from the volume V projected on the sky becomes

$$g(\gamma) = \frac{\sigma'\langle F_\nu\rangle^2}{2\pi\theta^2} \exp(-\gamma^2/2\theta^2),$$

where σ' is now the surface density of cluster centers per steradian. Finally, the power spectrum of the cosmic light from the volume becomes

$$s(\eta) = \frac{\sigma'\langle F_\nu\rangle^2}{4\pi^2} \exp(-\eta^2\theta^2/2).$$

But the mean cosmic-light intensity from this volume is $I_\nu = \sigma'\langle F_\nu\rangle$, so that the power spectrum may alternatively be written

$$s(\eta) = \frac{I_\nu^2}{4\pi^2\sigma'} \exp(-\eta^2\theta^2/2).$$

This relation is integrated along the line of sight in order to calculate the power spectral density of the total cosmic light. If the spatial covariance is the sum of a series of Gaussians, the power spectrum for each may be calculated independently and the results added at the end.

If the evolution of the covariance structure of the galaxy distribution along the line of sight is neglected (and we will have no choice at the present but to do so), the spectral density for a particular Gaussian spatial covariance may be scaled to deduce the power spectrum for any other Gaussian covariance. Suppose that for a density

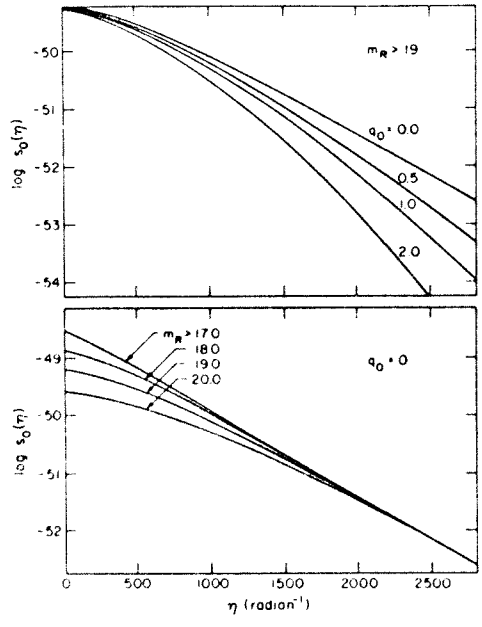

FIG. 4.—Standard cosmic-light spectral density at 6500 Å for a constant correlation length $l = 1$ Mpc and density contrast $\beta = 1$. Units are those of the text.

contrast $\beta = 1$ and a correlation length $l = 1$ the power spectral density is $s_0(\eta)$. Then for any other density contrast or correlation length

$$s(\eta) = \beta l^3 s_0(l\eta) .$$

Figure 4 presents the power spectrum of the cosmic light $s_0(\eta)$ for $\beta = 1, l = 1$ Mpc. At sufficiently high wavenumber $\eta = |\eta|$ the power spectrum differs markedly for different cosmological models. The minimum size effect prevents the generation of significant power at these small angular sizes.

The power spectrum is falling off so rapidly, however, that if in practice the spatial covariance is the result of a broad spectrum of correlation lengths, the contribution to the power spectrum from the shorter scales tends to mask the cosmological effects due to the longer clustering lengths. In this case the cosmic light is not clearly characterized by some minimum angular size.

The contribution to the power spectrum $s_0(\eta)$ from each increment along the line of sight is presented in figure 5. The spectral density is even more strongly localized in depth than the mean cosmic light. Again the regions of greatest interest lie between $z = 0.2$ and $z = 0.6$.

An estimate of the covariance structure of the distribution of galaxies in space is made from the correlation analysis of galaxy counts. Analyses of the Lick counts (Shane and Wirtanen 1967) have been made by Neyman *et al.* (1953) and Limber (1954) with very different results.

Table 4 presents the results of Neyman *et al.* in terms of the density contrast β and correlation length l, reduced to a Hubble constant $H_0 = 100$ km s^{-1} Mpc^{-1}. The outcome depends strongly on the assumed luminosity function, since distances to the counted galaxies are inferred from the mean absolute magnitude M_0 of galaxies counted to an apparent limiting magnitude m. The Gaussian luminosity function of

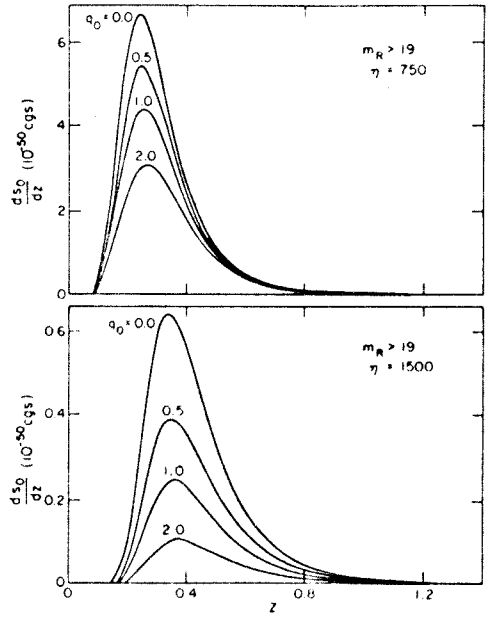

FIG. 5.—Differential contribution to the standard cosmic-light spectral density from the increment in redshift *dz*.

TABLE 4

COUNT ANALYSIS OF NEYMAN *et al.*

σ_m	$m - M_0$	β	l (Mpc)	σ_m	$m - M_0$	β	l (Mpc)
0.00.....	32.8	1.11	0.59	1.25.....	32.8	3.71	0.94
	33.8	1.16	0.89		33.8	3.45	1.37
	34.8	1.18	1.35		34.8	3.24	1.91
0.85.....	32.8	2.50	0.71	2.00.....	32.8	5.15	1.91
	33.8	2.58	1.07		33.8	5.25	2.54
	34.8	2.22	1.63		34.8	4.55	3.52

dispersion σ_m assumed by Neyman *et al.* bears little resemblance to that of Kiang. However, the volume-weighted luminosity function $\phi(M)10^{-0.6M}$ which results from the Kiang luminosity function is a fair approximation to that generated by a Gaussian luminosity function $\phi(M)$ of mean absolute photographic magnitude $M_0 = -18.3$ (corrected to the galactic pole) and dispersion $\sigma_m = 0.85$.

The distance modulus $m - M_0 = 36.6$ which results from an effective limiting magnitude, corrected for redshift, of $m = 18.3$ (Shane and Wirtanen 1967) lies outside the range of values considered by Neyman *et al.* An extrapolation of the results in table 4 yields

$$\beta = 2.0\,, \qquad l = 3.4 \text{ Mpc}\,.$$

Limber, on the other hand, arrived at a value for the density contrast $\beta \sim 25$ at correlation lengths $l > 4$ Mpc. Such a high covariance density would appear difficult to maintain over such large scales even if all galaxies occurred in rich clusters of the type catalogued by Abell (1958).

More recently Gunn (1965) has counted galaxies on a grid of considerably smaller angular size, with counting cells 10 arc minutes on a side, compared to 1° for the Lick counts. Although the luminosity function which Gunn used in interpreting the observed count correlation function exhibits the correct mean brightness, an underestimate of the mean density of galaxies in space necessitates a correction to the derived correlation length by a factor of 0.8. The finer angular scale of the counts revealed a short-range core to the spatial covariance, which was best fitted by a sum of three Gaussians:

$$\beta_1 = 36\,, \qquad l_1 = 1.2 \text{ Mpc}\,,$$

$$\beta_2 = 2.2\,, \qquad l_2 = 3.2 \text{ Mpc}\,,$$

$$\beta_3 = 2.7\,, \qquad l_3 = 8.0 \text{ Mpc}\,.$$

The term at the longest correlation length is likely to be an artifact due to systematic changes in the magnitude limit of the counts across the entire area of the single 48-inch (122-cm) Schmidt plate. The covariance in the middle range is very close to that derived by Neyman *et al.* Since the rms cluster population scales with l^3, the apparently large density contrast at the shortest correlation length does not conflict with estimates of the space density of rich clusters.

Figure 6 presents the power spectrum of the cosmic light $s(\eta)$ to be expected from the covariance density derived by Gunn. The term at 8.0 Mpc has been neglected but at any rate would not have affected the spectral density beyond $\eta \sim 300$ radian^{-1}. Roughly speaking, the cosmic light should exhibit rms fluctuations of about 20 percent at wavenumbers up to $\eta \sim 1000$ radian^{-1}. Although the cosmological dependence is

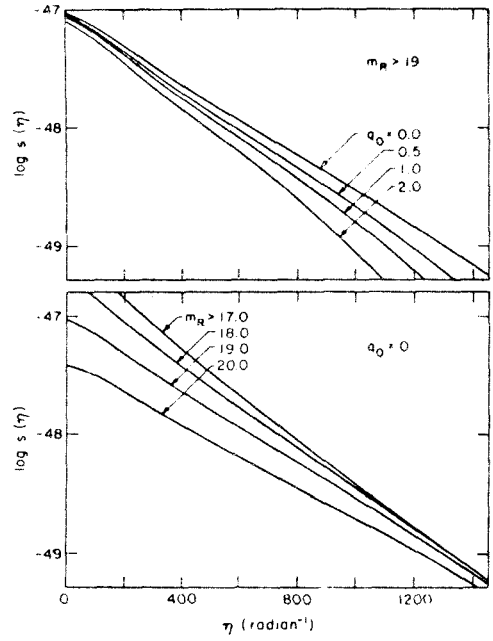

FIG. 6.—Predicted cosmic-light spectral density for the covariance density derived by Gunn.

quite modest, the spatial power spectrum of the cosmic-light distribution is a sensitive measure of the optical emissivity of the universe and of the distribution of galaxies in space.

VI. SINGULAR COMPONENT

In addition, the discrete nature of the galaxy distribution generates a singular contribution to the cosmic-light covariance density

$$g(\gamma) = \Omega^{-1} F_\nu^2 \delta(\gamma)$$

for each galaxy with observed flux F_ν in an area of the sky Ω. If $N(F_\nu)$ is the number of sources of brightness F_ν per steradian per unit brightness, then the singular component of the covariance

$$g(\gamma) = \delta(\gamma) \int F_\nu^2 N(F_\nu) dF_\nu$$

yields a white-noise component of the spectral density

$$s(\eta) = \frac{1}{4\pi^2} \int F_\nu^2 N(F_\nu) dF_\nu .$$

Table 5 presents the calculated white-noise spectral density due to the singular component of the galaxy distribution. Since most of the effect is due to the brightest galaxies in a sample, the variation with rejection magnitude is large. Compared to the spectral density expected from the continuous correlation of the galaxy distribution, the singular component is small but not negligible up to wavenumbers $\eta \sim 1000$ radian^{-1}.

TABLE 5

SINGULAR COMPONENT OF THE COSMIC-LIGHT SPECTRAL DENSITY
(10^{-50} ergs^2 s^{-2} cm^{-4} sterad^{-1} Hz^{-2})

	$m_R >$			
$q_0 =$	17.0	18.0	19.0	20.0
0.0.....	16.0	6.40	2.32	0.76
0.5.....	15.4	6.05	2.13	0.68
1.0.....	14.9	5.72	1.97	0.60
2.0.....	14.0	5.21	1.73	0.51

VII. ERROR ESTIMATES

Finally, we estimate the area of the sky which must be sampled in order to measure the spatial power spectrum of the cosmic light to a given accuracy.

The actual situation lies in between two extreme cases. Suppose that the number of clusters which generate most of the power at a given wavenumber is very small, so that the number of important clusters along the line of sight in any direction is rarely more than one. Then the observed spectral density in the sampled area will depend upon the number of clusters nature has seen fit to provide that area, in general not exactly the expected value. If, on the other hand, the number of clusters is very large, the resultant distribution of the cosmic light on the night sky approaches in character a formally Gaussian random process. For such a process the accuracy with which the power spectrum may be determined depends upon the number of linearly independent estimates of the spectral density which are available from a sample of given size.

Such linearly independent estimates are available at intervals in wavenumber $\Delta\eta = \pi/l$ for a one-dimensional record of length l and are called elements of the periodogram of the sampled data. For the cosmic light, a two-dimensional process, each estimate occupies an area in the plane $\Delta\eta_1\Delta\eta_2 = \pi^2/\Omega$, where Ω is the solid angle of the sample. Since the cosmic-light spectral density is expected to be circularly symmetric, let the periodogram be averaged over the arc $\eta_1^2 + \eta_2^2 = \eta^2$. Then for each value of the power spectrum determined with spectral resolution $\Delta\eta/\eta$ the number of independent elements of the periodogram available from a square sample area is

$$N = \frac{\Omega}{2\pi}\eta^2\left(\frac{\Delta\eta}{\eta}\right),$$

and the fractional standard deviation of the value is $N^{-1/2}$. For a spectral resolution $\Delta\eta/\eta = 0.25$ at wavenumber $\eta = 1000$ radian^{-1}, a sample area of 0.01 sterad would suffice to reduce the expected fractional error of the spectral density to 5 percent. Estimates based upon the assumption that the cosmic light resembles a Gaussian random process represent an effective lower limit to the expected error for the cosmic-light spectral density.

Now consider the expected error due to the uncertainty in the actual number of clusters present in a given sample area. Suppose that clusters of galaxies are randomly distributed in space. We do not wish to take a phenomenological stand on this issue but merely to make a simplifying assumption bearing some resemblance to the physical situation. In an increment of volume along the line of sight let the expected number of clusters of luminosity L per unit luminosity be $n(L)$. Imagine for just a moment that a cluster of luminosity L' generates a contribution to the cosmic-light spectral density $s'(\eta)$, and that all of the clusters have the same shape. Then from this volume the contribution to the power spectrum at wavenumber η will be, for clusters

of luminosity L,

$$ds(\eta) = s'(\eta)(L/L')^2 n(L)dL \pm s'(\eta)(L/L')^2 (n(L)dL)^{1/2} .$$

Evidently the fractional standard deviation for the spectral density from this increment will be

$$e = \frac{(\int s'^2(\eta)(L/L')^4 n(L)dL)^{1/2}}{\int s'(\eta)(L/L')^2 n(L)dL} .$$

If we let $N = \int n(L)dL$, then

$$e = N^{-1/2}\langle L^4\rangle^{1/2}/\langle L^2\rangle .$$

In order to estimate N, recall that for clusters independently distributed in space a density $\rho' = \rho\langle L^2\rangle/\langle L\rangle^2$ depends only on the density contrast and correlation length. In the volume under consideration let $N' = \rho' V$:

$$N' = N\frac{\langle L^2\rangle}{\langle L\rangle^2} = \frac{V}{(2\pi)^{3/2} l^3 \beta} .$$

Then the fractional error becomes

$$e = N'^{-1/2}\langle L\rangle\langle L^4\rangle^{1/2}/\langle L^2\rangle^{3/2} .$$

For a sample area of 1 sterad, let e_0 be the fractional standard error of the total cosmic-light spectral density (taking into account each increment along the line of sight) for a distribution of galaxies of unit density contrast and correlation length (Mpc), in clusters of uniform richness ($\langle L\rangle\langle L^4\rangle^{1/2}/\langle L^2\rangle^{3/2} = 1$). Because the contribution to the cosmic-light spectral density from each increment of distance is distributed differently with wavenumber, the standard deviation e_0 varies with η. For some other distribution of galaxies in space the expected error for a sample of solid angle Ω becomes

$$e(\eta) = \frac{\beta^{1/2} l^{3/2}}{\Omega^{1/2}} e_0(l\eta) \frac{\langle L\rangle\langle L^4\rangle^{1/2}}{\langle L^2\rangle^{3/2}} .$$

In our approach to the characterization of clusters of galaxies there is some ambiguity in that the covariance may be characterized by more than one density contrast and correlation length. Fortunately, for the covariance density arrived at by Gunn the coefficient $\beta^{1/2} l^{3/2} \simeq 10$ for both the term at $l = 1.2$ Mpc and that at $l = 3.2$ Mpc.

The coefficient $\langle L\rangle\langle L^4\rangle^{1/2}/\langle L^2\rangle^{3/2}$ is a measure of how strongly the cosmic-light spectral density is concentrated in the richest clusters. For the distribution in richness of the clusters catalogued by Abell (1958) this factor is 1.6. Even if Abell clusters generated all of the cosmic-light spectral density while accounting for only 1 percent of the galaxy counts, this number would be at most 16. More realistically we estimate $3 < (\langle L\rangle\langle L^4\rangle^{1/2}/\langle L^2\rangle^{3/2}) < 10$.

Figure 7 presents the results for $e_0(\eta)$. At the largest angular scales the power is generated by relatively few nearby clusters resulting in a larger expected standard error. For a sample area of 0.01 sterad and the covariance density deduced by either Neyman *et al.* or Gunn, $e(\eta) \sim 10^3 e_0(l\eta)$. For the cosmic-light spectral density of figure 6 a standard deviation as high as $\sim$20 percent might be anticipated in the neighborhood of $\eta = 1000$ radian^{-1}, somewhat greater than that expected for a Gaussian random process.

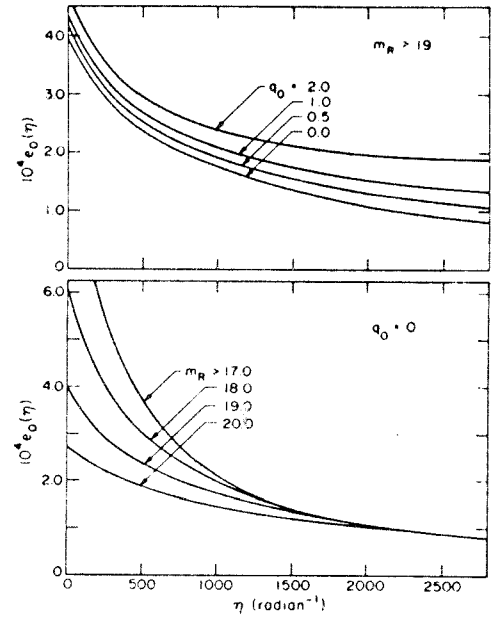

FIG. 7.—Standard fractional error of the cosmic-light spectral density for a constant correlation length $l = 1$ Mpc and density contrast $\beta = 1$, in a sample area $\Omega = 1$ sterad. The error is only that part due to the statistical deviation of the number of clusters in a given sample area from the expectation value.

Note that since a given cluster of galaxies contributes power to the cosmic-light spectral density over a range of angular scales, the actual error due to the variation in the number of clusters in a given sample area will tend to be correlated through some range of wavenumber. The expected error $e(\eta)$ differs in this important respect from that due to a Gaussian random process.

Although the background light due to distant galaxies is expected to be only a small fraction of the total nightsky intensity, one expects the cosmic light to be strongly modulated by the clustering of galaxies in space. In a minimum sample area of 0.01 sterad, we expect the power spectrum of the cosmic-light fluctuations to convey considerable information regarding the distribution of galaxies in space and the luminosity density of the universe.

It is a pleasure to thank Professor J. E. Gunn for the valuable guidance he has provided throughout the course of this investigation. The author gratefully acknowledges the support of a National Science Foundation Graduate Fellowship. This work was supported in part by National Science Foundation grants GP-27304 and GP-28027.

REFERENCES

Abell, G. O. 1958, *Ap. J. Suppl.*, 3, 211.
———. 1962, in *Problems of Extragalactic Research*, ed. G. C. McVittie (New York: Macmillan), p. 213.
Christensen, C. 1968, preprint.
Gunn, J. E. 1965, Dissertation, California Institute of Technology.
Holmberg, E. 1958, *Medd. Lunds Obs.*, Ser II, No. 136.
Hubble, E. 1936, *The Realm of the Nebulae* (New Haven: Yale University Press).

Humason, M. L., Mayall, N. U., and Sandage, A. R. 1956, *A.J.*, **61**, 97 (HMS).
Kiang, T. 1961, *M.N.R.A.S.*, **122**, 263.
Limber, D. N. 1954, *Ap. J.*, **119**, 655.
Neyman, J., Scott, E. L., and Shane, C. D. 1953, *Ap. J.*, **117**, 92.
Oke, J. B., and Schild, R. 1970, *Ap. J.*, **161**, 1015.
———. 1971, *ibid.*, **169**, 209.
Sandage, A. R. 1961, *Ap. J.*, **133**, 355.
Sandage, A. R., and Tammann, G. 1964, *Carnegie Yrb.*, p. 35.
Shane, C. D., and Wirtanen, C. A. 1967, *Pub. Lick Obs.*, Vol. **22**, Pt. 1.
Shapiro, S. 1971, *A.J.*, **76**, 291.
Zwicky, F. 1957, *Morphological Astronomy* (Berlin: Springer-Verlag).

PART TWO

THE SMALL SCALE ANISOTROPY OF THE COSMIC LIGHT

I. INTRODUCTION

Because galaxies cluster in space, the cosmic background light due to galaxies is not smoothly distributed on the night sky. In a previous paper (Shectman 1973, Paper I), we showed that the spatial power spectrum of the cosmic light is a sensitive measure of the distribution of galaxies in space and of the luminosity density of the universe.

The cosmic light fluctuations arise from galaxies at redshifts from z=0.2 to z=0.6. For clustering on the scale of one megaparsec, the fluctuations appear at an angular scale of a few minutes of arc. The predictions of Paper I for the cosmic light fluctuations are based on the luminosity function for nearby galaxies and on the clumpiness of the galaxy distribution derived from galaxy counts. The rms amplitude of the cosmic light anisotropy is expected to be on the order of 20 percent of the mean cosmic light, but only one part in 2000 of the total brightness of the night sky at 6500 Å.

We have measured the spatial power spectrum of the cosmic light on a series of photographic plates taken with the Palomar 48-inch (122 cm) Schmidt camera. The specific intensity of the cosmic light fluctuations was calibrated using a photoelectric exposure meter and spot sensitometry

of the photographic emulsion. The plates were digitized using a computer-controlled microphotometer.

It is important to exclude from the measured anisotropy two effects unrelated to clusters of galaxies. The first of these arises from individual stars and galaxies in the range of magnitude $m_R \lesssim 18$. These objects generate a white noise component of the cosmic light power spectrum which masks the contribution from clusters of galaxies. The second effect is due to the extended scattering halos around bright stars, which mimic the appearance of clusters of galaxies.

When these effects have been dealt with, the fluctuations in the data due to irregularities in emulsion and development are distinguished from those due to distant clusters of galaxies on the assumption that the emulsion noise is essentially uncorrelated from plate to plate of the same field. A series of control plates exposed in the telescope through a diffusing screen gives us some confidence in this procedure.

The resultant power spectrum of the cosmic light is finally interpreted to provide a measure of the covariance of the galaxy distribution and the mean emissivity of galaxies in space.

II. PLATE MATERIAL

26 Eastman 103a-F (backed) plates were exposed on the nights of 1971 March 1,29,30 and 31, and April 22 and 23. All of the plates were taken of the same field at galactic latitude ℓ=+82.5 deg centered on the star

SAO 063499 $\alpha = 13^h\ 19^m\ 54^s.9$ $\delta = +30°\ 33'\ 13''$ (1950.0).

This field was chosen on Palomar Sky Survey prints as the closest area east of the galactic pole which is 1) free of bright stars and galaxies, 2) clear of the Coma cluster of galaxies and 3) near the zenith when on the meridian at Palomar.

Each plate was exposed for 40 minutes through the Schott RG-1 filter, under optimum photometric conditions. For none of the plates did the zenith distance at mid-exposure exceed sec(z)=1.23. 17 of the plates were 10x10 inches in size, and 9 were 14x14, but the size of the RG-1 filter limited the useable area of the larger plates to that of the 10x10's. Each plate was developed for 9 min in MWP-2 developer using the rocker agitation machine. The same solutions were rarely used to develop more than 3 plates.

In order to generate a group of control plates to check on systematic effects in the observational material the telescope was covered with a full-aperture diffusing screen. 7 plates were exposed through the RG-1 filter with the dome

closed, using artificial illumination. At least one such plate was exposed from every box of 6 plates on each night the telescope was in use. These control plates were developed along with the sky plates following each observing session.

An effort was made to remove the plates from their boxes and insert them in the plateholder with nearly random rotations of 90°. Moreover, the filter can be mounted in the telescope in one of 4 orientations, which was changed and recorded for each plate. The plates were run through the development process with nearly random rotations of 90°. In this way we sought to avoid any systematic small-scale irregularities in emulsion or development. The known orientation of the filter for each exposure allows the explicit measurement of any systematic effect from this source.

III. CALIBRATION

The calibration of each plate consists of two parts. A photometer measures the incident intensity of the night sky for each plate. Spot sensitometry calibrates small changes in the transmission of the plate in terms of small fluctuations in the sky brightness.

The photometer consisted of a 2-inch diameter achromat

of 10-inch focal length which imaged the sky on an aperture 1/2-inch in diameter. A filter of red plexiglas and 1 mm of Schott BG38 defined the bandpass. The field lens of a standard Mount Wilson cold box imaged the objective on the S-20 photocathode of an ITT FW-130 photomultiplier. An SSR amplifier-discriminator fed the signal to a GR counter. The accumulated counts in selected 10-second intervals were recorded at the beginning, middle and end of each exposure by the observer or night assistant on forms prepared for this purpose. The count rate on the night sky was typically 3000 sec^{-1}.

The pointing of the entire assembly was adjusted until the field coincided roughly with that of the 48-inch Schmidt. The precise field boundaries were then defined by moving the 48-inch in the vicinity of a bright star. In use, the response of the exposure meter at five points in its field was calibrated by observing the star α Boo several times each night. The extinction coefficient was taken to be α=0.09 mag, after Oke (1965). On the night of 1971 April 22, α Boo and α Lyr were observed in succession, tying the calibration to that of Oke and Schild (1970).

In order to convert the calibration of the flux from a standard star to the intensity of the night sky, one must know the equivalent aperture of the system on the sky. The geometric measurements of the system imply an aperture

2.64 deg in diameter, while a scan across the aperture with a bright star yields a value of 2.75 deg. We have adopted a value of 2.70 deg which we feel is unlikely to be in error by more than 3 percent.

Figure 1 shows the relative spectral sensitivities of the exposure meter and the photographic system, together with a scan of the night sky taken by J.E. Gunn on the 200-inch telescope with the multichannel spectrophotometer during the spring of 1971. The response of the RG-1 filter, with a measured thickness of 2.24 mm, and the response of the 103a-F emulsion were obtained from Schott and Kodak handbooks respectively. The exposure meter filter was measured in the laboratory while the S-20 photocathode sensitivity is taken from specifications by ITT. Because the exposure meter maintains an appreciable response beyond 7000 Å where the sky becomes very bright, a correction of approximately 7 percent is required to convert the intensity derived in the photoelectric passband to that of the photographic plate. The photographic band is centered on wavelength 6490 Å. Both bands are equally sensitive to the [OI] spectral feature at 6300 Å which is highly variable in the night sky.

A final correction to the nightsky intensity is required to account for the contribution of starlight in the exposure meter field. No stars are present in the field

which can contribute individually as much as one percent of the observed intensity. The contribution of the numerous faint stars has been derived from data by Roach and Negill (1961), assuming an average correction from the visual to the photored band of 0.4 mag (relative to the flux from α Lyr). The stellar contribution amounted to 0.3×10^{-18} erg $sec^{-1}cm^{-2}sterad^{-1}Hz^{-1}$ (for simplicity let us call these cgs units). The derived intensity of the night sky for each plate ranged from 3.31 to 5.94×10^{-18}cgs, with a mean of 4.55×10^{-18}cgs. The total systematic error in the determination of the incident intensity for each plate is expected to be less than 10 percent.

Since the cosmic light fluctuations are small perturbations on the background density of each plate, we require simply the contrast

$$\gamma(T) = - \frac{d(\log T)}{d(\log I)}$$

at the mean photographic transmission (T) for each plate.

On each of the 7 plates exposed through the diffusing screen, and on 3 of the 14 X 14-inch plates of the sky, an area in the corner of each plate was masked during exposure. Using a spot sensitometer with an incandescent light source filtered by red plexiglas, a series of spots of increasing intensity was exposed for 30 minutes in each of these masked areas, after the plates were exposed in the telescope.

The nominal value for the interval of intensity in the spot sequence is $I_{n+1}/I_n=\sqrt{2}$. However, we have found that the ratio of intensity between particular spots varies from this value by typically ±10 percent. The intervals in exposure between spots were calibrated on a plate with four sets of spots at four different settings of the lamp intensity, taken by J.E. Gunn 1971 May 24. The intensity intervals between spots were adjusted so as to minimize the residuals of the overall calibration curve for all four sets of spots. On other plates of this kind taken subsequently we have found that these corrections are fairly stable for several months, but then change considerably, evidently when the optical components of the spot machine are cleaned.

The spots on each of the 10 plates were measured using the same optical set-up which was used to digitize all of the plates. The transmission of each spot was integrated over a central square 895μ on a side (1 arc min at the plate scale of the 48-inch Schmidt). Figure 2 presents the results from 9 plates for the contrast $\gamma(T)$, in the range of transmissions of interest. The data for one plate with severe plate defects have been omitted. For each pair of spots adjacent in intensity, we have plotted the value

$$\gamma_n = - \log(T_{n+1}/T_n)/\log(I_{n+1}/I_n)$$

at the density

$$D = -0.5(\log T_{n+1} + \log T_n) \quad .$$

The range of density lies at the toe of the photographic calibration curve, where the contrast is rising rapidly. We found that $\gamma(T)$ is remarkably stable from plate to plate, even though the sensitivity (the constant of integration required to convert the function $\gamma(T)$ into a relation between density and specific intensity) varies markedly among the plates.

The curve shown in Figure 2 is a polynomial fit to the contrast as a function of density for 9 plates. We have applied this curve to all of the plates to derive for each the contrast at the measured value of the background density. The contrast for the sky plates ranges from 0.88 to 3.83. The mean contrast was 2.16. For the ensemble of 26 plates the systematic error in the photographic calibration should not exceed 3 percent.

IV. MEASUREMENT

All of the plates were digitized using a two-axis computer controlled scanning microphotometer. A Raytheon 703 computer with 4K words of core memory issues commands to a pair of stepping motor controllers which drive the X and Y

motions of a rebuilt Eichner iris photometer. The iris can be replaced with a slit which illuminates an area of the plate and is re-imaged at the field lens of a photomultiplier tube. An electrometer connected to the photomultiplier output drives a v-f converter connected to a counter. The computer can gate the counter open or closed, read and reset the counter in response to timing interrupts generated by a quartz crystal clock. Periodically the computer dumps a buffer-full of data on 9-track magnetic tape.

In use the computer was instructed to execute a 256-line raster scan of each plate. The stage was advanced 895μ each time the machine completed a row and started back in the other direction. Each row was somewhat longer than the width of a 10 X 10-inch plate to allow the image of the slit to traverse an area of clear stage and cross the edge of a steel rule which provided both a fiducial point and a measure of the photomultiplier dark current for every row. The stage was driven along each row at a rate of 417 5μ steps each second, and the count from the v-f converter with a peak frequency of 100 KHz was read every 16 msec. The size of the rectangular slit projected on the plate was 20μ in the direction of motion along each row by 895μ. Each raster scan required 9 hours to complete and generated approximately 2 million words of data.

All of the plates, including the 7 fogged plates, were

measured in the order in which they were exposed. In addition, every seventh measuring session was run with no plate at all, just the blank glass stage of the microphotometer. This stage was scrupulously cleaned before every one of the forty 9-hour measuring sessions, twice each day.

Each plate was placed with the same orientation, emulsion down at the center of the stage. The guide star at the center of the plate provided the reference position for the registration of each row from plate to plate. The rotation of the plate relative to the X and Y axes was adjusted using a selected star near one edge of the field. The position of the guide star displayed by up-down counters attached to the stepping motors was checked at the beginning and end of each run to guarantee that the machine had advanced the proper distance for each row. In this way we are confident that the position of each raster scan is coincident on all of the plates to within 50μ.

For permanent storage the data tape for each run was copied onto high density 1600 bpi tape, using the IBM 370/155 with which all of the data reduction was accomplished. At the same time the order of the data was reversed for every other row to compensate for the alternating direction of motion of the raster scan. The dark count, clear stage response, and fiducial point were determined for each row.

Next a program compared the positions of the fifty brightest stars traversed by the slit for each row with the positions on a standard data set. The plates had been aligned well enough that the positions of these stars in each data record were coincident to $\pm 30\mu$ with those on the adopted standard plate. The fiducial marks generated by the steel rule on the standard data set allowed an offset of $\sim 60\mu$ to be applied for play between the motions of the stage in alternating directions.

During the twenty day period in which the plates were measured the machine ran continuously without failure. Not one of the 80,000 records of output data failed to be read successfully. At this point the data for each plate consisted of 6875 X 256 useful measures of the transmission of the photographic emulsion, each of area 1 arc min by 2.2 arc sec, covering a field 256 arc min (=9.00 inch) square at the center of each plate.

V. MAGNITUDE CUT-OFF

As discussed in Paper I, it is necessary to eliminate from the data the light from those stars and galaxies brighter than some given red apparent magnitude (we will always refer to magnitude relative to the flux from α Lyr in the red band). These objects generate a large white noise

component to the cosmic light power spectrum which is of no cosmological significance and which carries little information regarding the distribution of galaxies in space. Moreover, the signal to noise ratio of the final result deteriorates for brighter rejection limits as the white noise begins to swamp the power from distant clusters of galaxies.

The signature of a bright star or galaxy is the sudden change in the transmission of the emulsion as the analyzing slit scans across the image. For a given object the change in transmission is set by the area of the seeing disk, and by the response of the photographic emulsion to varying intensity.

By the seeing disk we really mean the response to a point image of the photographic plate, telescope and atmosphere in combination. We have measured this seeing transfer function by scanning with a small (0.5 X 2.0 arc sec) slit across the diffraction spikes of the guide star at the center of the field. The natural width of the diffraction spike is expected to be negligible compared to the widening due to imperfections in the emulsion, telescope and atmospheric seeing. The northern and western spikes were measured for the guide star on each plate. The transmission of the emulsion at each position of the slit was converted to intensity and the resulting profile fitted

to a Gaussian of the form $\exp(-x^2/2\sigma^2)$. The resulting values for σ ranged from 1.5 to 4.4 arc sec, with an average value of 2.2 arc sec. The standard deviation for the measurement on each plate was 0.3 arc sec.

Using the photographic calibration and this Gaussian seeing profile we have calculated the change in transmission of each plate in response to stars of varying magnitude. The intensity of the seeing image at many points was converted to transmission of the photographic emulsion. The total change in transmission was calculated for an area 4.4 arc sec X 1 arc min, the sum of two successive data points in the raster scan. The results for two plates at the extremes of seeing and emulsion contrast are shown in Figure 3. When the images become gray near the plate limit the change of transmission is always linear in the incident flux, while the contrast sets the constant of proportionality.

The grain noise in each measure of the transmission sets a limit to the brightness of a star which can be reliably distinguished against the mean local transmission of the plate. In our case this limit is near magnitude 18 and in practice was chosen to be $m_R=18.1$.

For galaxies the original image is not a perfect point and we can expect the results to differ from those for stars. Fortunately galaxies of eighteenth magnitude are in general

not very much larger than the seeing disk. We have performed separate calculations for the change in transmission expected from both elliptical and spiral galaxies of varying magnitude and surface brightness. The profiles for elliptical galaxies were adopted from Oemler (1973) and those for spirals from Freeman (1970). The profiles were convolved with the derived seeing transfer function for 5 plates selected to represent the range of seeing and emulsion contrast.

Near magnitude 18 we found that the brightness of an elliptical galaxy was typically within 0.2 mag of that for a star at the same change in transmission of the analyzing area, while a spiral galaxy was typically within 0.1 mag. Since the interpretation of the cosmic light power spectrum does not depend strongly on the magnitude cut-off, we have chosen to ignore this small effect rather than to become ensnared in the complexities of taking suitable averages over inclination and surface brightness, for which the distributions are only approximately known.

In order to implement the magnitude cut-off, one requires a measure of the local background transmission across each plate. We arrived at this function by averaging the data from the raster scan along each row to form a 256 X 256 array of transmissions covering the field, and subsequently combining this array in 4 X 4 blocks to arrive

at a reduced 64 X 64 array of elements 4 arc min square. During this step any element of the intermediate 256^2 array which was grossly different ($0.05\gamma T_0$) in transmission from its neighbors was passed over in arriving at the background transmission in that neighborhood. In the rare instance that more than half of the constituent elements of a member of the 64^2 array were passed over, the entire box was declared a loss and its value assigned by smoothing over the 8 members of the 64^2 array immediately adjacent. The values of this array are adopted as the measure of the local background transmission for each plate.

At this point the adjacent members of each row of 6875 elements were summed two at a time to form an array of 6874 overlapping measures of the transmission of the photographic emulsion 4.4 arc sec by 1 arc min. This improves the signal to noise ratio for the magnitude cut-off since the seeing disk is on the order of this width. Any element of this smoothed array which differed from the local background transmission by more than some critical amount, and which caused a local minimum in the transmission, was taken to mark the position of an object brighter than the rejection magnitude limit. To set this critical level the plates were grouped with the 5 plates described above which cover the range of seeing and contrast for all the plates. For the rejection limit of 18.1 mag the critical change in

transmission ranged from 4.8 to 7.0 percent of the mean transmission of the plate.

For each element of the smoothed array which exceeded the critical residual transmission, 6 members of the unsmoothed array bracketing the position of the triggered element were discarded in arriving at a new 64^2 measure of the background transmission. Thus for each object brighter than the rejection limit an area of the field at least 5 arc sec on either side of the true position of the object was passed over. Again, when more than 180 of the 430 constituent elements of a member of the 64^2 array were unsuitable the value was derived by smoothing over the adjacent area.

In general, the new values for the plate background are slightly improved during this step, because of the finer spatial resolution and deeper rejection magnitude limit relative to the initial determination of the background. Since the same rejection is applied to data points which either exceed or fall short of the background transmission, the magnitude cut-off also effectively eliminates plate defects such as pinholes or smudges in the emulsion.

Using the improved values for the background transmission the magnitude cut-off is repeated using the identical method except that the values of the transmission of each

plate are compiled into a 256 X 256 array. No value is assigned to an element of the 256^2 array if more than 15 of the 27 data points which comprise it are eliminated by the magnitude cut-off.

The histogram of the residuals of the data against the background transmission for a typical plate are shown in Figure 4. For the 4.4 arc sec X 1 arc min residuals shown at the top the grain noise dominates, but a small asymmetric tail is generated by individual stars and galaxies. The boundaries of the figure are coincident with the rejection limit. A Gaussian fit to the distribution indicates that the magnitude cut-off is applied at the 3.61σ level of the scatter in the data. The average value of this figure for all of the plates was 3.63σ. When the data are averaged into the 256^2 array, for which the residuals are shown at the bottom of Figure 4, most of the grain noise disappears to reveal that any systematic drift in the level of the magnitude cut-off across the plate cannot exceed 10 percent.

The number of objects rejected on each plate averaged 21,500 for the 26 plates, with 20 of the plates in the range 19,000 to 23,000. The scatter is mostly due to the sensitivity of the rejection magnitude to the size of the seeing disk and the contrast for each plate, which are not perfectly uniform in each of the 5 groups of plates for which the value of the cut-off was calculated. For two

plates taken in exceptionally bad seeing some 27,500 objects were rejected. The 120,000 or so elements of the raster scan rejected on each plate still represent only 7 percent of the data.

Of the 21,500 objects detected on each plate perhaps one tenth are in fact plate defects or objects counted in more than one row of the raster scan. From counts of stars by Weistrop (1971) and of galaxies by Oemler (1973) we expect to find at least 12,200 stars (assuming an average correction from the visual to the photored of 0.6 mag at magnitude 18) and 2,300 galaxies, taking into account the dispersion in the magnitude cut-off caused by the scatter of the data. In view of the uncertainties in the counts in the red band at these magnitudes, we do not regard the discrepancy in number to be significant.

From the scatter in the 4.4 arc sec X 1 arc min data and the expected change in transmission of the analyzing area as a function of magnitude, one can calculate the probability that an object of given brightness survives the magnitude cut-off. Even when an object does survive, all of its light is not necessarily registered since in measuring the transmission of the plate in a large aperture a burned-out image produces little more effect than an image barely as bright as the sky background. As the images become fainter near the plate limit a greater proportion of

the light is recorded. Typically this efficiency ranges from 78 percent for a star of magnitude 18 to 96 percent at magnitude 20.

For each of the 26 plates we have calculated both the spread in the magnitude cut-off and the efficiency with which the light from stars of given brightness is recorded. The product of these two effects gives the fraction of the light registered in the data for objects of various magnitude, after the magnitude cut-off has been applied. Figure 5 presents the results for all 26 plates averaged together. Light from stars at m_R=17.5 is almost completely rejected while light from stars at m_R= 19.0 is almost completely accepted. The half-power point shifts from the original 18.1 mag to m_R= 18.2. Again we do not expect the results for galaxies to differ systematically from those for stars by as much as 0.2 mag.

VI . STAR HALOS

At this point the data are nearly ready to analyze for the cosmic light fluctuations. However, the extended scattering halos around the brightest stars in the field generate fluctuations which resemble distant clusters of galaxies. Fortunately, the bright star at the center of each star halo enables one to deal with this effect explicitly, under the

assumption that all the halos have the same shape and that the brightness of each halo is proportional to the flux from the central star.

Figure 6 shows one quadrant of the halo surrounding the star SAO 082706 (m_R=3.7), averaged in circular arcs. This star is not in the field analyzed for the cosmic light but is accessible in the corner of the field of the 14 X 14 inch plates. The halo was measured on one plate using essentially the same technique outlined above but with a raster scan of 15 arc second spacing. The halo approximately follows an inverse-square law to at least 6 arc min, though beyond this a small change in the adopted background density of the plate can alter the slope somewhat. The bump at log r=0.65 is an optical effect in the telescope but is not strong enough to prevent one from dealing with an idealized power-law halo. The structure at larger radii is caused by noise in the data, to which no magnitude cut-off has been applied. Fluctuations of the relevant angular size are generated largely in the region from r=1 to 10 arc min.

Using a computer analysis to predict the power spectrum generated by the star halos we arrived at a two-fold scheme for removing them from the data. Within a radius ranging from 5.5 arc min for the brightest stars in the field (m_R=6.3) to 2.3 arc min for stars of m_R<11.2, the data in the 256 X 256 array are simply discarded. The radii are chosen

to optimize the suppression of the star halo power spectrum while keeping the loss of data to a minimum. Some 7000 one arc min square elements or 11 percent of the data are rejected in this step. Outside of this radius a small correction is applied to the data on the basis of photometry of each star.

In order to generate a finding list for the bright stars in the field, the data from four plates before the application of the magnitude cut-off were summed to form a 256^2 array. In both the X and Y directions the data were summed two at a time to form an array of overlapping elements 2 arc min on a side. A list was generated of all elements of the array whose transmission deviated from the background by more than a specified value and which caused a local minimum in the transmission. Summing the data two at a time prevented the loss of stars which by chance lay on the boundary between elements. A number of galaxies were eliminated by inspection of the field, leaving a list of 334 stars, to which a few bright stars just beyond the edge of the field were added.

In one night with the Palomar 60-inch telescope, photoelectric magnitudes were obtained in the red band for the 82 brightest stars on the list and for 62 stars from the remainder. These latter served as standards for iris photometry on one plate of all the stars on the list. Comparison

of the measured magnitude with the residual transmission which caused each star to be included in the list indicates that the photoelectric sample is complete to magnitude 9.8. The sample with iris photometry is complete to magnitude 10.8 while substantially (at least 80 percent) complete to m_R= 11.2. The photometric sample includes 233 stars brighter than 11.2 mag.

Using the data in 256 X 256 arrays before application of the magnitude cut-off, the strength of the inner halo (log r=0.3) was measured on all 26 plates for the two brightest stars in the field. The halo appears to be constant on all of the plates to within the error of the measurement, about 10 percent.

A list was compiled of all the elements of the 256^2 array, 7152 in number, to be discarded because of proximity to a bright star. In addition, a 256 X 256 array of corrections for star halos (m_R<11.2) to the intensity in the field was generated. Armed with this information the analysis of the data after the magnitude cut-off is ready to proceed.

VII. FURTHER REDUCTION

On the data for 26 plates the positions of the elements of the 256 X 256 arrays for which no value was assigned

after the magnitude cut-off were compared. For the sake of uniformity no element was used on any of the plates for which no value was available on more than four plates. Since the magnitude cut-off corresponds to a different increment of intensity for each plate, it is not surprising that some elements were eliminated on only a few plates. A total of 1491 elements not already on the list of those too close to bright stars were eliminated in this step.

At this point the data arrays for each plate were converted to intensity using the photoelectric and photographic calibrations, and all were summed together. The corrections for star halos were applied to the data, which were summed in 4 X 4 blocks to arrive at a 64 X 64 array. A plot of this array revealed that most of the values in the northernmost row of data were systematically bright by some 0.2 percent of the sky brightness, evidently due to an edge effect on some of the plates. The data in this row of the 64^2 array were discarded for the rest of the analysis. None of the other edges revealed any significant systematic effect.

A circular average of these data about the center of the field showed the expected vignetting of the 48-inch telescope, for which the primary mirror is too small to fully illuminate the corners of a 10 X 10-inch plate. The radial intensity profile is nearly flat to a radius of 2 deg

as seen on the sky, but then falls abruptly, reaching a deficiency of 2 percent at a radius of 3 deg in the very corner of the field. A correction for this radial profile was applied to all of the data in the subsequent analysis.

The data in this 64^2 array were smoothed over an area of 9 points to arrive at an accurate estimate of the local background intensity across the field. Figure 7 shows the histogram of the residual intensity for the data in the summed 256 X 256 array against this background. Again note the asymmetric tail which is largely due to elements of the array coincident in position with one or a few stars of moderate brightness or with the fringes of bright galaxies. A final 582 elements with residuals greater than 0.5 percent of the brightness of the night sky were placed on the list of points to be excluded from the data before analysis for the cosmic light fluctuations. The exclusion level of 0.5 percent is still a factor of 10 larger than the expected rms fluctuations of the cosmic light.

Finally the data for each plate after the magnitude cut-off were summed in 4 X 4 blocks, omitting the 9225 points on the list of elements to be excluded. In addition, from 65 to 886 elements containing unique plate defects had been eliminated on each plate during the magnitude cut-off. No value in the 64 X 64 array for each plate was assigned when the values for fewer than 8 elements in the

more detailed array were available. Estimates of the intensity were omitted for fewer than 10 percent of the elements in each 64 X 64 array. At last the data are ready to be analyzed for the cosmic light fluctuations.

VIII. POWER SPECTRA

The statistical character of the cosmic light fluctuations is expressed in terms of the spatial power spectrum of the distribution of intensity on the night sky. The power spectrum is essentially the contribution to the variance of the data from fluctuations of angular scale characterized by the wavenumber η.

Power spectrum analyses were performed on the data in 64 X 64 arrays of elements 4 arc min square, using a standard fast Fourier transform routine. Prior to the analysis any element of a data array for which no value was available was assigned a value by smoothing over the 8 adjacent members of the array. As long as the number of missing elements is not large the effect of this smoothing on the spectral density can be neglected. The mean value of the intensity is subtracted to avoid an enormous peak at zero wavenumber and the resultant power spectrum $s(\eta)$ is normalized so that

$$\langle \Delta I^2 \rangle = \int s(\underset{\sim}{\eta}) d^2\underset{\sim}{\eta}$$

where ΔI is the intensity distribution with mean removed.

The integral extends over all four quadrants of the wavenumber $\underset{\sim}{\eta}$. The units of $s(\underset{\sim}{\eta})$ are $ergs^2s^{-2}cm^{-4}sterad^{-1}Hz^{-2}$.

Since the power spectrum is expected to be circularly symmetric, the spectral density is averaged in circular arcs about zero wavenumber to obtain a spectrum in $\eta=|\underset{\sim}{\eta}|$ for which

$$\langle \Delta I^2 \rangle = \int s(\eta)(2\pi\eta)d\eta \quad .$$

An exception to the assumption of circular symmetry is caused by instrumental drift during the digitization of each plate. Since the motion of the raster scan is very rapid along each row but on average quite slow from one row to the next, changes in the sensitivity of the apparatus appear largely as plane waves propagating from row to row. Nearly all of the power generated by this process shows up in the one row of the power spectrum for which $\eta_x=0$. We do not expect this drift to be correlated from plate to plate. Nevertheless the signal to noise ratios of the resultant spectra are enhanced by omission from the circular average of those values of the spectral density for which $\eta_x=0$. For reasons which will become apparent we have also omitted those values of the power spectrum for which $\eta_y=0$. The loss of data is not serious except for very low values of the wavenumber η.

Before proceeding with the analysis of the cosmic light fluctuations, we wished to check the validity of the cor-

rections to the data for the intensity in star halos. The results are shown in Figure 8. The solid line is the power spectrum of the corrections for the halos of stars brighter than magnitude 11.2. The spectrum is quite steep since discarding the data in the core of each star halo is an effective low-pass filter. The open circles are the amount of power that disappears from the data when the corrections for star halos are applied. The agreement is quite good until the value of the spectral density is low enough to be both unimportant and difficult to measure. The dashed line is the calculated residual power in the data due to the halos of stars fainter than magnitude 11.2. A correction for this small residual spectral density is applied to the subsequent power spectra.

The data in their final form contain a significant amount of power caused by irregularities in the photographic emulsion. We distinguish the power in emulsion noise from that due to the cosmic light fluctuations on the expectation that the positions of only the cosmic light fluctuations are correlated from plate to plate. The intensities for all 26 plates are added up and the power spectrum which results contains both emulsion noise and the cosmic light fluctuations. Then the data are added up with one of 8 random orientations for each plate; four rotations by 90° and a choice of parity. The power from the emulsion noise which

was random to begin with is unaffected, but the power in the cosmic light is reduced to only 1/8 of its proper value. The power that disappears is correlated from plate to plate and is assigned to the cosmic light.

In practice the spectral density for random orientations of the data is determined for 9 trials with different random orientations of the 26 plates. The random orientation for each plate is chosen so that all 8 orientations are used once before any are used twice, and so on. The values of the spectral density for which $\eta_y=0$ must be omitted from the circular average, since for some of the random orientations the sense of the x and y axes is interchanged.

Figure 9 presents the results for the spatial power spectrum of the cosmic light. The open circles are the power in both emulsion noise and cosmic light fluctuations, for all 26 plates lined up correctly. The filled circles are 8/7 of the power that disappears when the orientations are chosen at random. Both spectra are corrected for the residual star halo power for $m_R>11.2$. The original two-dimensional power spectra were circularly averaged at 128 values of the wavenumber η and 8 of these estimates were combined to provide each point shown in the figure. The formal error bars are based on the standard deviation of the 8 constituent elements for each point, but assuming that only 64 independent estimates of the spectral density were

present in the original circular average.

When the plates were added together with the same orientation as the filter for each exposure no power appeared at an upper limit which could cause even a 1 percent contamination of the observed power spectrum for wavenumbers $\eta \geq 400$ radian^{-1}. Since the filter positions are already distributed through 4 of the 8 random orientations of the data, only 1/8 of the filter spectral density can appear in the observed power spectrum of the cosmic light. The correlated spectral density present in the data taken with no plate at all on the stage of the microphotometer does not contaminate the data at greater than the 1 percent level.

Of the 7 plates taken through the full-aperture diffusing screen one was rejected entirely due to severe plate defects. No significant correlated spectral density was observed in the remaining 6 plates but the upper limits are not as low as one might hope because of the small number of plates. The value of the upper limit ranges from 0.5 of the observed cosmic light spectral density at $\eta=800$ radian^{-1} to 0.1 at $\eta>1500$. Since the optical configuration of the Schmidt camera is nearly constant over scales on the plate equivalent to a few minutes of arc, it is implausible that the telescope itself contributes appreciably to the observed power spectrum. In order to generate a spectral density as

great as 10^{-48} at η=500 radian^{-1} would require, for instance, an rms mottling of the reflectivity of the mirror on the order of 20 percent at scales of 0.6 inch.

Implicit in the assertion that the observed anisotropy of the night sky brightness is due to distant clusters of galaxies is the assumption that no other effects correlated on the sky produce fluctuations of comparable intensity. We have had to deal explicitly with one such effect, due to the halos of the brightest stars on the plate. A number of other processes have been considered but appear to be too small to generate an appreciable contribution to the observed power spectrum.

Internal reflections in the Schmidt camera produce the familiar "ghosts" opposite the positions of the bright objects on the plate. But even on a red plate of Aldebaran (m_R=0.1) the ghost does not exceed 20 percent of the nightsky intensity. Since the brightest stars in the field analyzed for the cosmic light are 300 times fainter than α Tau (there are only 5 within a factor of 1000), the ghosts cannot generate the observed spectral density.

Patchy obscuration near the north galactic pole is surely too weak to modulate the cosmic light at the observed 20 percent rms level. Measurements of the color excess at the galactic poles have exhibited a secular decrease with time. Most recently McClure and Crawford (1971) have found

E(B-V)=0.00 mag±0.01, and Feltz (1972) has measured E(b-y)= 0.000mag±0.002. More serious is the reflection of galactic starlight by patchy obscuring material. The surface brightness of the Milky Way is some 60 times that of the expected mean cosmic light, but even if the obscuring material is taken to have an albedo of 1, the observed anisotropy becomes difficult to produce at such low values for the color excess. A contour plot of the data for 26 plates breaks up into a jumble of contours at the level of .002 of the mean sky brightness. No conspicuous objects are evident and so just a few strongly obscured patches will not do.

Could the observed anisotropy be associated with extended emission from the nearby field galaxies on the plate? The brightest galaxy in the area surveyed for the cosmic light is the elliptical NGC 5127, (m_R=12.3) which exhibits the most conspicuous extended image of any galaxy on the plate. Still, at a radius of 3 arc min the surface brightness of this galaxy is only 0.5 percent of the mean nightsky brightness on the 26 plates. This is a factor of 17 less than the intensity at 3 arc min of the halos of the brightest stars in the field. We conclude that the observed anisotropy is not associated with nearby field galaxies. The most likely hypothesis remains that the observed cosmic light power spectrum is indeed generated by distant clusters of galaxies.

IX. THE COVARIANCE OF THE DISTRIBUTION OF GALAXIES IN SPACE

Finally, we would like to interpret the observed cosmic light anisotropy as it appears on the sky in terms of the three-dimensional distribution of galaxies in space. Our approach to this problem has been treated in detail in Paper I.

If the function $F(\underset{\sim}{r})$ is the probability density that a galaxy exists at $\underset{\sim}{r}$, and $\varepsilon(\nu)$ is the mean volume emissivity of galaxies, then $\varepsilon(\nu)F(\underset{\sim}{r})$ is the probable emissivity at the point $\underset{\sim}{r}$ in space. For the galaxy-light distribution $\varepsilon(\nu)F(\underset{\sim}{r})$ the covariance density

$$G(\underset{\sim}{x}) = \frac{\varepsilon^2(\nu)}{V} \int_V F(\underset{\sim}{r})F(\underset{\sim}{r}+\underset{\sim}{x})\,d^3\underset{\sim}{r}$$

describes the correlation from one point in space to the next of the probability that a galaxy exists. The covariance density $G(\underset{\sim}{x})$, together with a cosmological model, is sufficient to predict the observed cosmic light power spectrum $s(\eta)$.

In particular consider the covariance expanded in a series of Gaussians

$$G_i(\underset{\sim}{x}) = \beta_i \varepsilon^2(\nu) \exp(-x^2/2\ell_i^2) \quad .$$

The density contrasts β_i are the ratios $\langle F^2 \rangle / \langle F \rangle^2$ for clustering at correlation lengths ℓ_i. As demonstrated in Paper I, the cosmic light power spectrum is linear in the different Gaussian terms and obeys the scaling law

$$s_i(\underset{\sim}{\eta}) = \beta_i \ell_i^3 s_o(\ell_i \eta)$$

where $s_o(\eta)$ is the spectral density generated by clustering with a density contrast $\beta=1$ at a correlation length $\ell=1$.

Sample cosmic light power spectra for Gaussian spatial covariances of correlation length $\ell=2.5$, 1.0 and 0.4 Mpc were predicted using exactly the same recipe described in Paper I. The spectral density scales with $\varepsilon^2(\nu)$. From the luminosity function for nearby galaxies an emissivity $\varepsilon_o(\nu)$ is adopted according to the treatment of Paper I. The magnitude cut-off was taken to be that of Figure 5.

The amplitudes of these spatial covariances, together with a white noise term for individual stars and galaxies beyond the rejection limit, were adjusted to produce a least-squares fit to the data of Figure 9. The fit for deceleration parameter $q_o=0$ has been drawn through the points together with its decomposition into

individual Gaussian terms. The arrow indicates the level of the white noise (12.9×19^{-50} in cgs units). The values of the density contrast of the galaxy distribution for this case are

$$\beta_1 = 5.3 \pm 7.8 \quad , \quad \ell_1 = 2.5 \text{ Mpc}$$

$$\beta_2 = 29 \pm 4.8 \quad , \quad \ell_2 = 1.0 \text{ Mpc}$$

$$\beta_3 = 49 \pm 12 \quad , \quad \ell_3 = 0.4 \text{ Mpc}$$

The formal errors are the standard deviations for each value of the density contrast due to the errors in the observations s_j,

$$\sigma^2(\beta_i) = \sum_j \left(\frac{\partial \beta_i}{\partial s_j}\right)^2 \sigma^2(s_j)$$

calculated while holding fixed the other parameters of the fit. Because of the low weights of the first two points in the observed power spectrum the value of the density contrast at the longest spatial scale is only an upper limit. The value of the spatial covariance is best determined near 1 Mpc, at wavenumbers as seen on the night sky high enough for the errors of the observed power spectrum to be of reasonable size but low enough to prevent the white noise term from dominating.

The covariance density of the distribution of galaxies in space,

$$G(\underset{\sim}{x})/\varepsilon_o^2 = \sum_{i=1}^{3} \beta_i \exp(-x^2/2\ell_i^2)$$

which results from this fit is shown in Figure 10, with its decomposition into three Gaussian terms. For comparison, we also show the derived covariance for $q_o=2$ ($\beta_1 = 16\pm18$, $\beta_2 = 37\pm9$, $\beta_3 = 107\pm11$). The tentative covariance density

derived by Gunn (1965) from correlation counts of galaxies lies in between the curves for $q_o=0$ and $q_o=2$. The covariance density in either case resembles a power law of index -1.25 in the range of correlation length near 1 Mpc. The lengths are referenced to a Hubble constant $H_o=100$ Km sec^{-1} Mpc, but the density contrasts β_i are independent of the choice of H_o.

As a measure of the aggregate properties of the distribution of luminous material in the universe, the small scale anisotropy of the cosmic light is of value because of its freedom from obvious selection effects. Except for the relatively controlled rejection of bright galaxies in the survey area, the cosmic light power spectrum is sensitive to the spatial distribution of all luminous material in a volume of the universe of truly cosmological scale.

That the observed power spectrum of the cosmic light resembles so closely that which one expects on the basis of the luminosity function of nearby galaxies is evidence that these galaxies are substantially representative of the luminous material of the universe as a whole. The prospect of improved correlation counts of galaxies in the future opens the possibility of defining the volume emissivity of matter in the universe with considerable precision.

REFERENCES

Feltz, K.A. 1972, P.A.S.P., 84, 497.

Freeman, K.C. 1970, Ap. J., 160, 811.

Gunn, J.E. 1965, Dissertation, California Institute of Technology.

McClure, R.D. and Crawford, D.L. 1971 A.J., 76, 31.

Oemler, A. 1973, Ap. J., 180, 11.

Oke, J.B. 1965, Ann. Rev. Astr. Ap., 3, 23.

Oke, J.B. and Schild, R. 1970, Ap. J., 161, 1015.

Roach, F.E. and Negill, C.R. 1961, Ap. J., 133, 228.

Shectman, S.A. 1973, Ap. J., 179, 681.

Weistrop, D.E. 1971, Dissertation, California Institute of Technology.

FIGURE CAPTIONS

Fig. 1.- Relative spectral sensitivities of the photographic and photoelectric systems. The cosmic light anisotropy is measured in the photographic band but calibrated in the photoelectric band. The specific intensity of the night sky rises steeply beyond 7100 Å.

Fig. 2.- Contrast γ as a function of emulsion density from spot sensitometry of 9 plates. The curve is a polynomial fit to the data.

Fig. 3.- Calculated change in transmission of the photographic emulsion as a function of apparent stellar magnitude. The analyzing area is 4.4 arc sec X 1 arc min. Case I is for poor seeing and high emulsion contrast; case II for good seeing and low contrast.

Fig. 4.- Histograms of the data residuals against the background transmission for a typical plate. Top, residuals for the data in elements 4.4 arc sec X 1 arc min. The magnitude cut-off is applied to these data starting at the boundaries of the figure, at the 3.61σ level for the scatter in the data. Bottom, residuals for the data in elements 1 arc min square, after the magnitude cut-off. The scatter is reduced to one-tenth of the rejection limit.

Fig. 5.- Calculated total fraction of light registered in the data as a function of apparent magnitude, after

application of the magnitude cut-off.

Fig. 6.- Radial profile of the star halo for SAO 082706 (m_R=3.7). The line is a power law of index -2.

Fig. 7.- Histogram of the residual intensity of the data for all 26 plates in 1 arc min square cells.

Fig. 8.- Star halo power spectra. Solid line, power spectrum of the corrections to the data for the halos of stars of m_R<11.2. Open circles, observed decrease in spectral density when the corrections are applied to the data. Dashed line, calculated residual power spectrum generated by the halos of stars of m_R>11.2.

Fig. 9.- Observed cosmic light power spectrum. Open circles, power in fluctuations both correlated and uncorrelated from plate to plate. Filled circles, power generated by the correlated component only. The fit to the data is for 3 Gaussian covariance terms at correlation lengths ℓ=2.5, 1.0 and 0.4 Mpc (also shown individually). Arrow indicates the least squares fit to the white noise.

Fig. 10.- Covariance density of the distribution of galaxies in space. The solution for q_o=0 is shown composed of 3 Gaussian terms for correlation lengths ℓ=2.5, 1.0 and 0.4 Mpc.

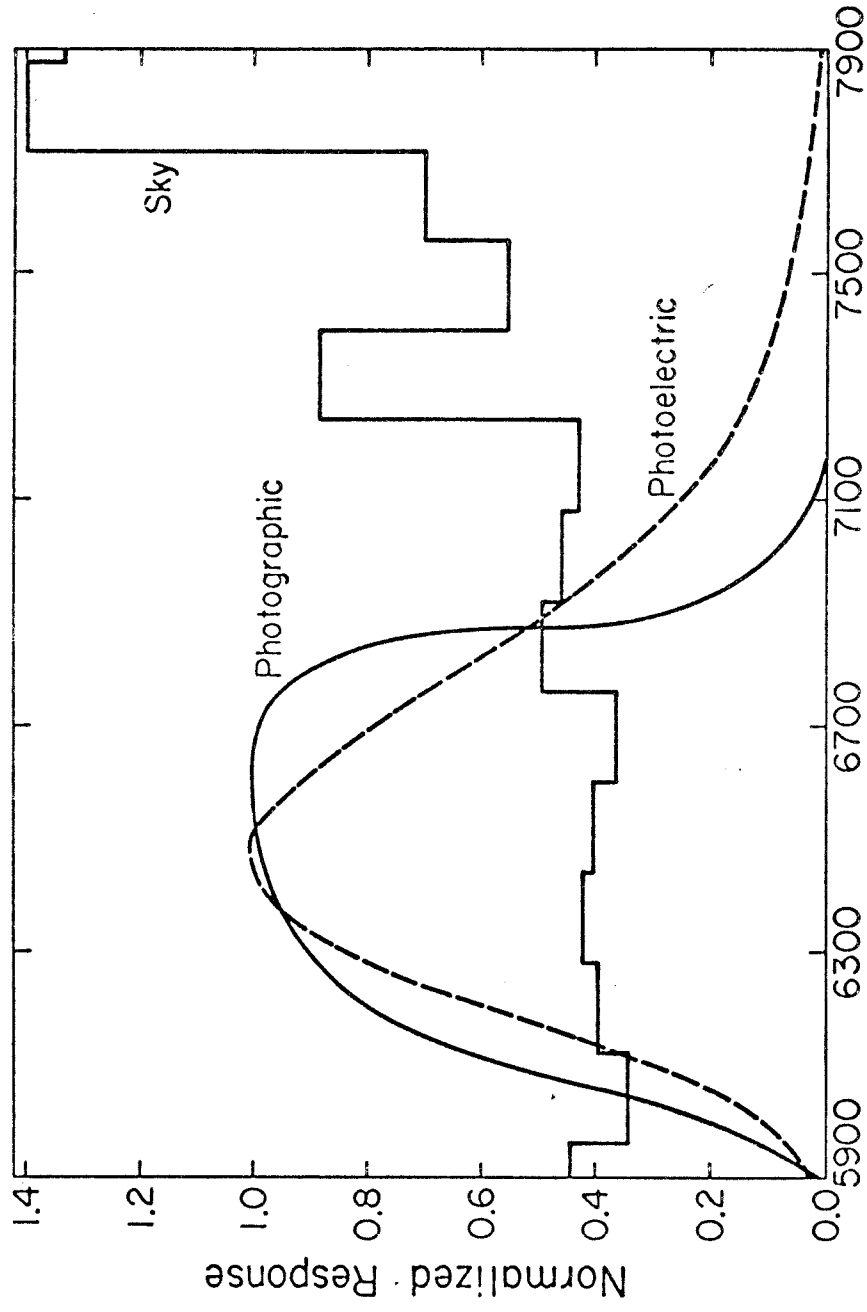

FIGURE 1.- Relative spectral sensitivities of the photographic and photoelectric systems. The cosmic light anisotropy is measured in the photographic band but calibrated in the photoelectric band. The specific intensity of the night sky rises steeply beyond 7100Å.

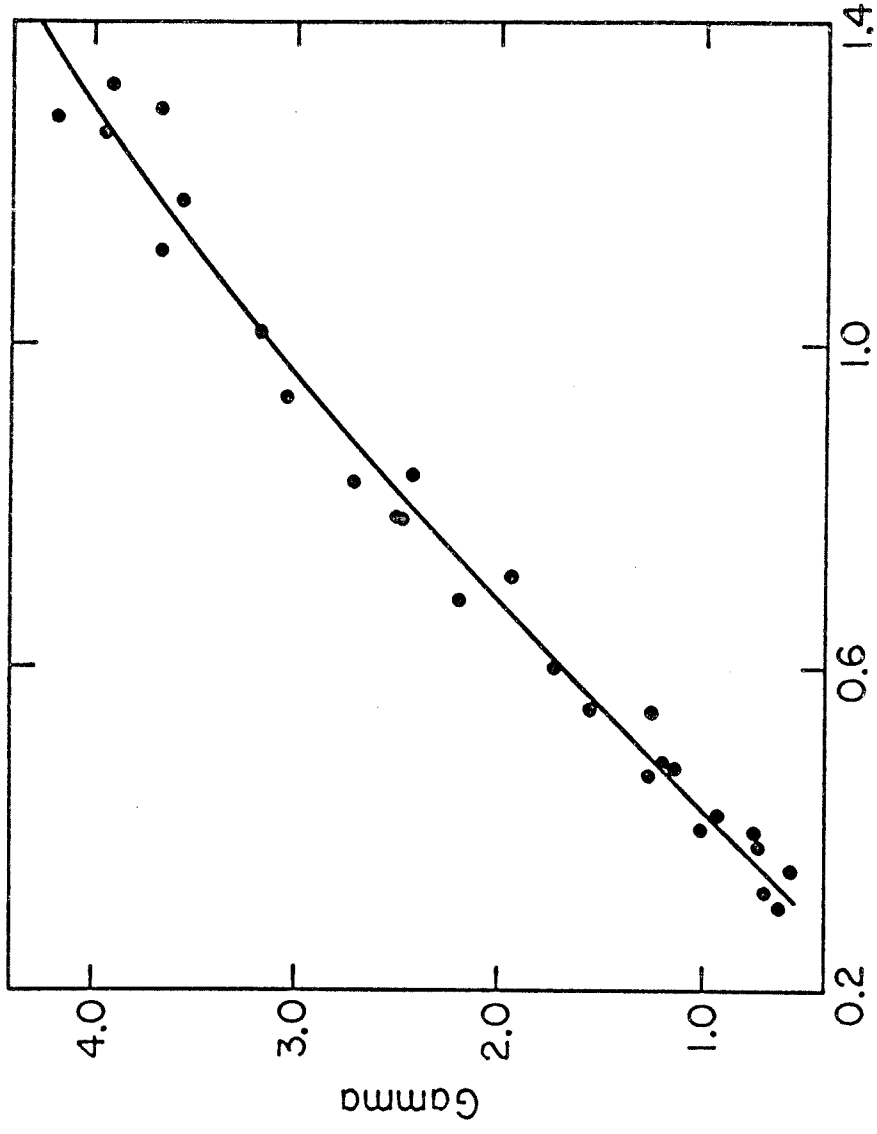

FIGURE 2.- Contrast γ as a function of emulsion density from spot sensitometry of 9 plates. The curve is a polynomial fit to the data.

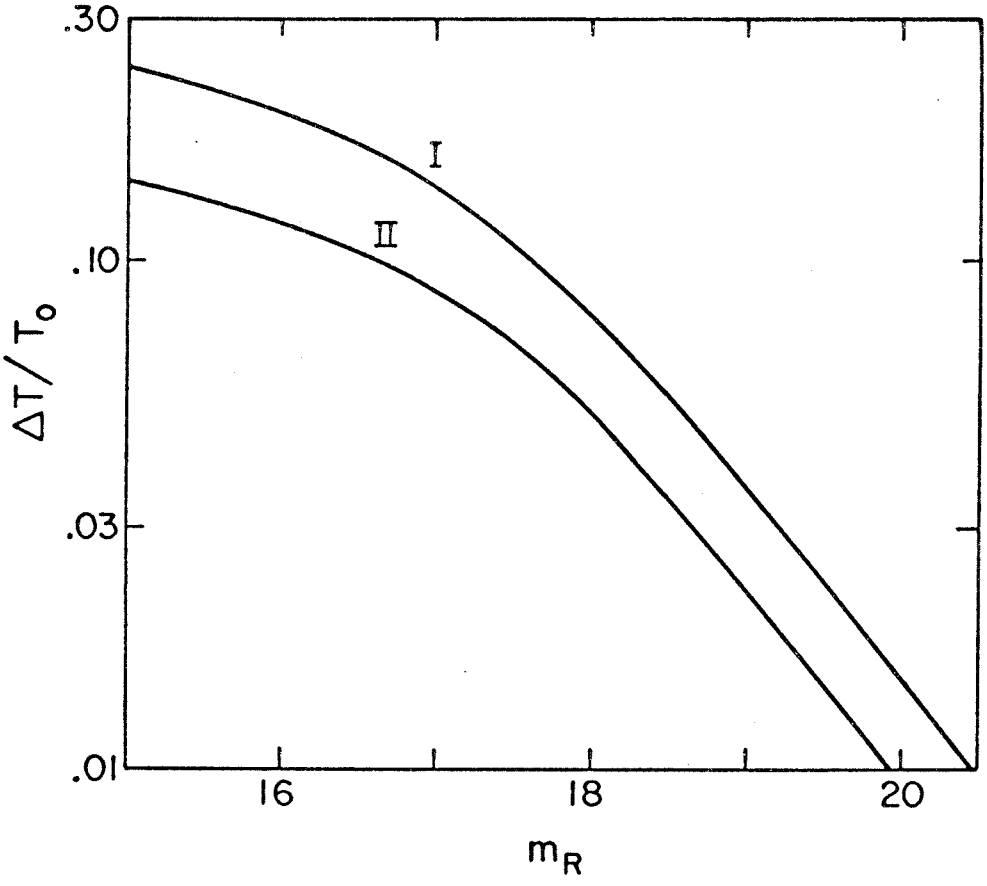

FIGURE 3.- Calculated change in transmission of the photographic emulsion as a function of apparent stellar magnitude. The analyzing area is 4.4 arc sec X 1 arc min. Case I is for poor seeing and high emulsion contrast; case II for good seeing and low contrast.

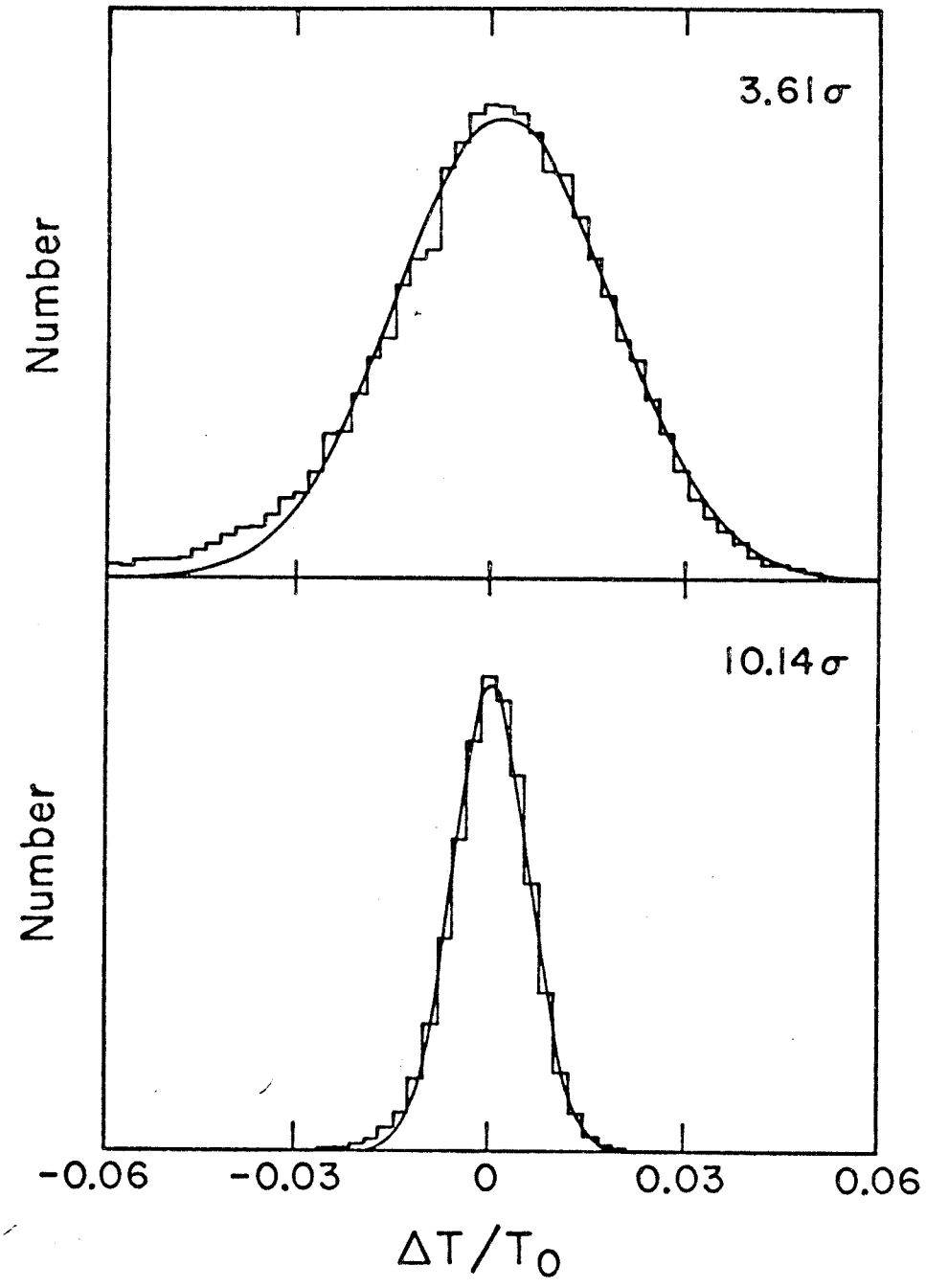

FIGURE 4.- Histograms of the data residuals against the background transmission for a typical plate. Top, residuals for the data in elements 4.4 arc sec X 1 arc min. The magnitude cut-off is applied to these data starting at the boundaries of the figure, at the 3.61σ level for the scatter in the data. Bottom, residuals for the data in elements 1 arc min square, after the magnitude cut-off. The scatter is reduced to one-tenth of the rejection limit.

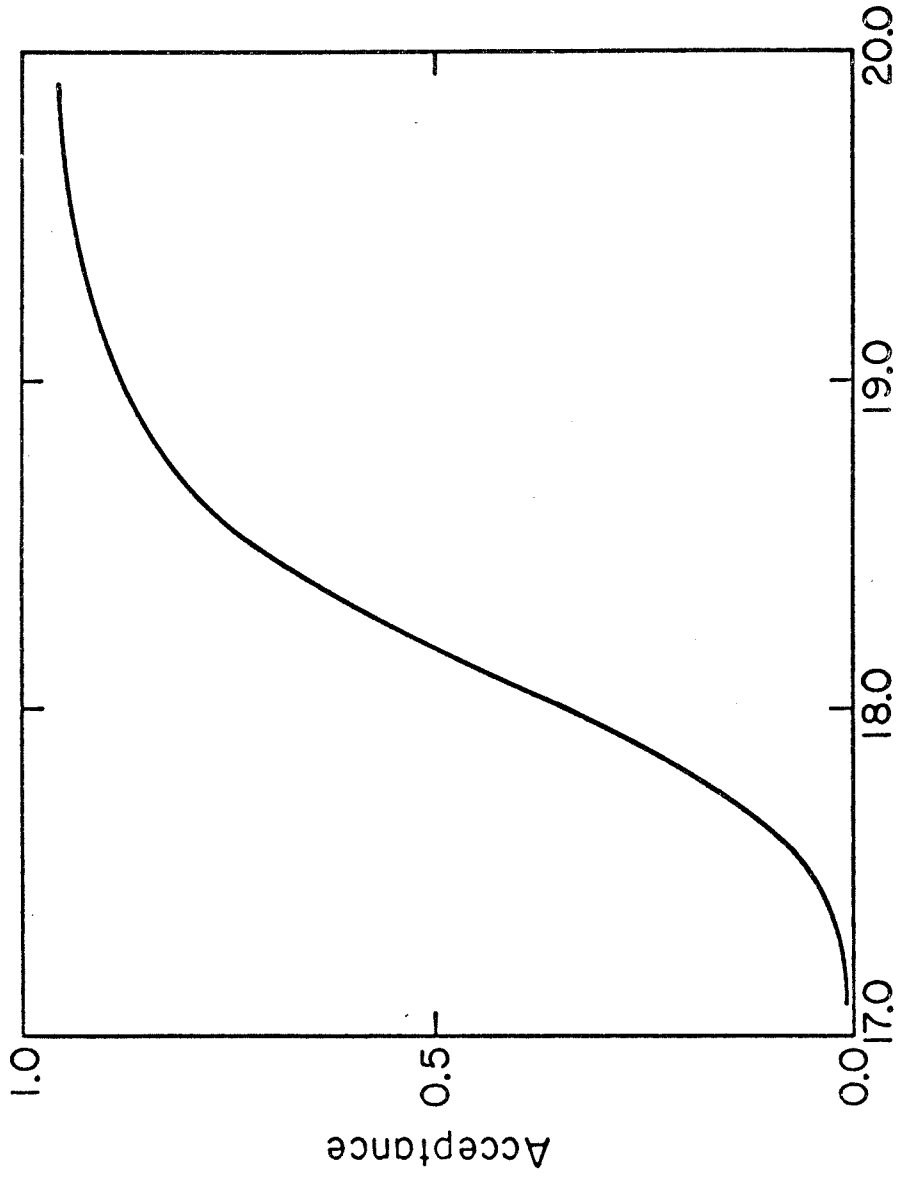

FIGURE 5.- Calculated total fraction of light registered in the data as a function of apparent magnitude, after application of the magnitude cut-off.

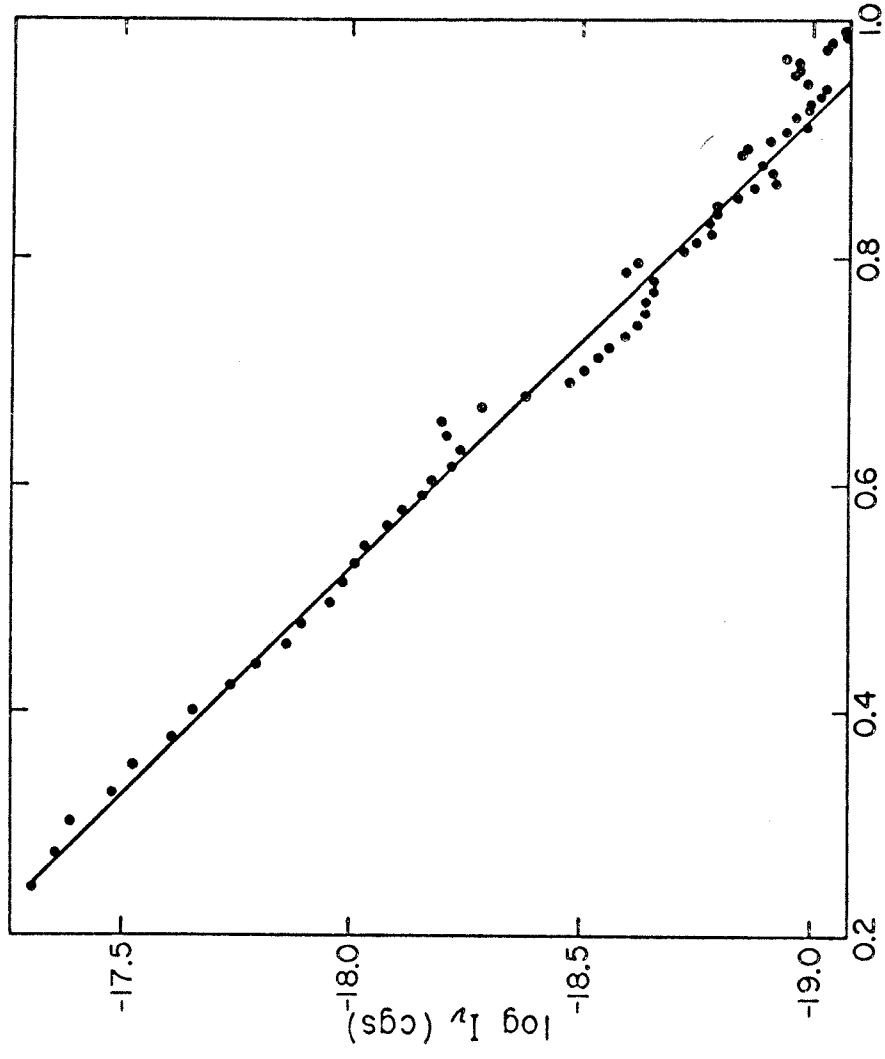

FIGURE 6.- Radial profile of the star halo for SAO 082706 (m_R=3.7). The line is a power law of index -2.

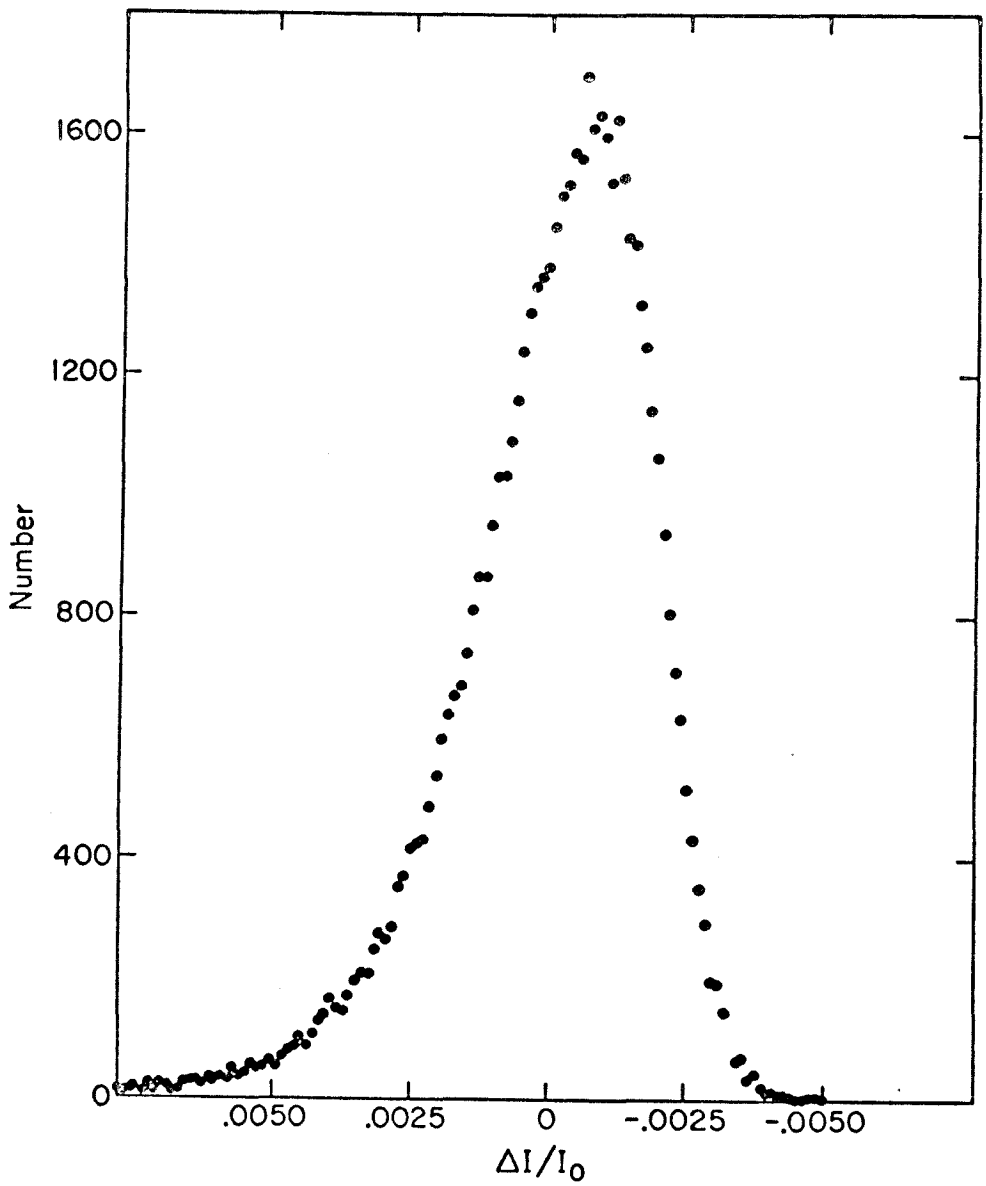

FIGURE 7.- Histogram of the residual intensity of the data for all 26 plates in 1 arc min square cells.

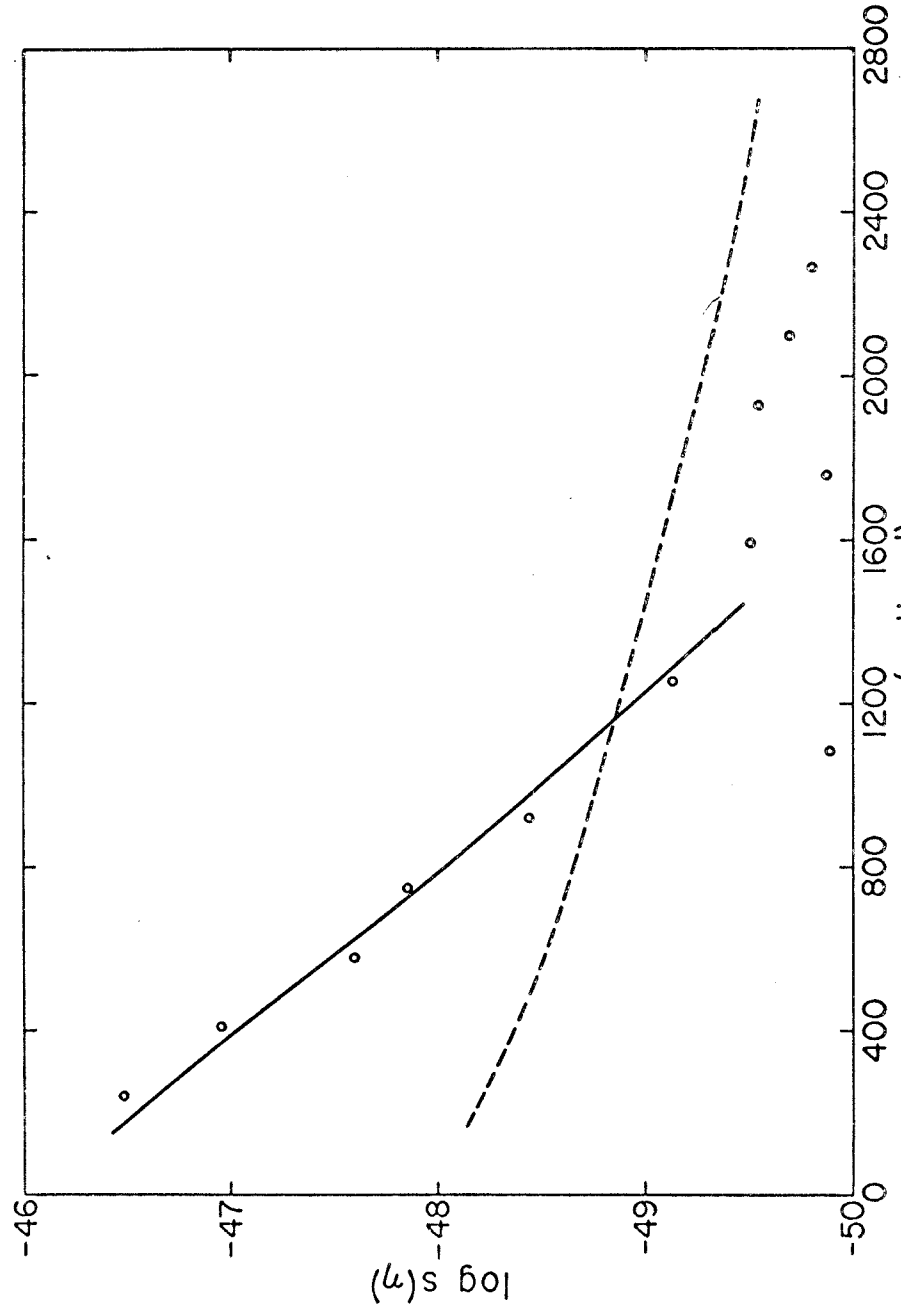

FIGURE 8.- Star halo power spectra. Solid line, power spectrum of the corrections to the data for the halos of stars of $m_R<11.2$. Open circles, observed decrease in spectral density when the corrections are applied to the data. Dashed line, calculated residual power spectrum generated by the halos of stars of $m_R>11.2$.

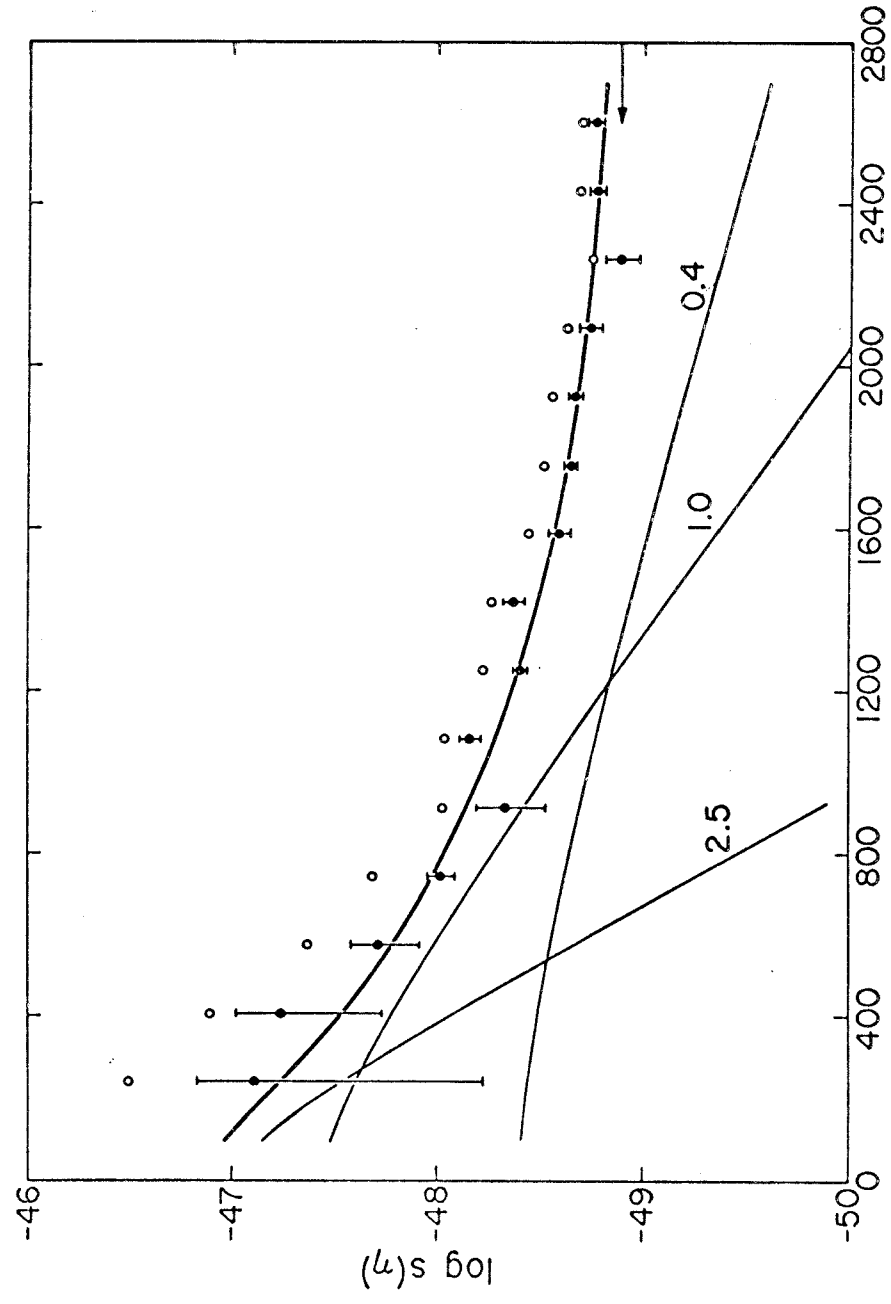

FIGURE 9.- Observed cosmic light power spectrum. Open circles, power in fluctuations both correlated and uncorrelated from plate to plate. Filled circles, power generated by the correlated component only. The fit to the data is for 3 Gaussian covariance terms at correlation lengths ℓ=2.5, 1.0 and 0.4 Mpc (also shown individually). Arrow indicates the least squares fit to the white noise.

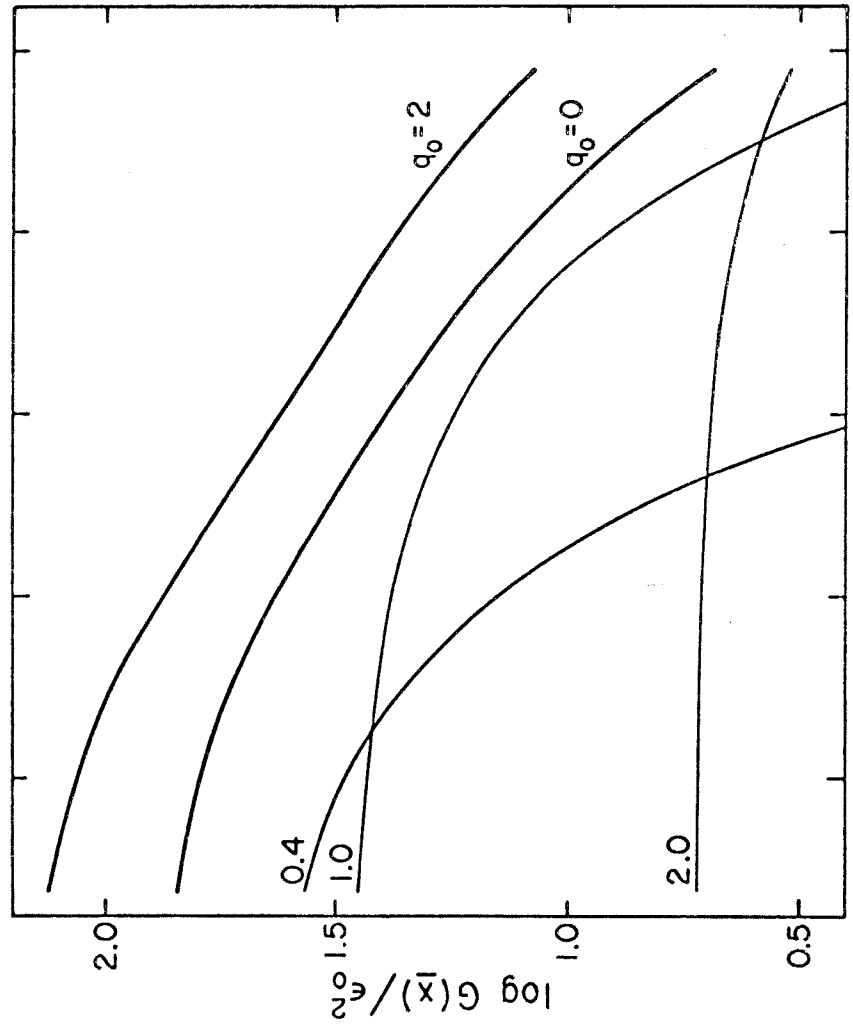

FIGURE 10.- Covariance density of the distribution of galaxies in space. The solution for $q_o=0$ is shown composed of 3 Gaussian terms for correlation lengths ℓ=2.5, 1.0 and 0.4 Mpc.